이학박사 학위논문

Low Cholesterol level in CAP1-Knockout mice: CAP1 is an essential binding partner of PCSK9 to degrade LDLR

PCSK9 이 LDL receptor 의 재활용을 억제하는데 에는 CAP1 과의 결합이 필수적 이다: CAP1 결손쥐 분석의 결과

2017 년 08 월

서울대학교 대학원
분자의학 및 바이오 제약학과
양 지 민

A thesis of the Degree of Doctor of Philosophy

PCSK9 이 LDL receptor 의 재활용을 억제하는데 에는 CAP1 과의 결합이 필수적 이다: CAP1 결손쥐 분석의 결과

Low Cholesterol level in CAP1-Knockout mice: CAP1 is an essential binding partner of PCSK9 to degrade LDLR

August 2017

Dept. of Molecular Medicine and
Biopharmaceutical Sciences
Seoul National University
Jimin Yang

PCSK9 이 LDL receptor 의 재활용을 억제하는데 에는 CAP1 과의 결합이 필수적이다: CAP1 결손쥐 분석의 결과

지도 교수 김 효 수

이 논문을 이학박사 학위논문으로 제출함
2017년 7월

서울대학교 대학원
분자의학 및 바이오 제약 전공
양 지 민

양지민의 이학박사 학위논문을 인준함
2017년 6월

위 원 장 _____ (인)

부위원장 _____ (인)

위 원 _____ (인)

위 원 _____ (인)

위 원 _____ (인)

Low Cholesterol level in CAP1−Knockout mice: CAP1 is an essential binding partner of PCSK9 to degrade LDLR

By
Jimin Yang

A thesis submitted to the Department of Molecular Medicine and Biopharmaceutical Sciences in partial fulfillment of the requirements for the Degree of Doctor of Philosophy in Convergence Science and Technology at Seoul National University College

July 2017

Approved by Thesis Committee:

Professor _____Chairman

Professor _____Vice chairman

Professor _____

Professor _____

Professor _____

ABSTRACT

Introduction: Proproteinconvertase subtilisin/kexin type 9 (PCSK9) regulates low density lipoprotein receptor (LDLR) expression on liver cells mediating its lysosomal degradation. Therefore, PCSK9 has emerged as an important target of lowering LDL-cholesterol and also treatment of atherosclerotic cardiovascular diseases. However, the precise mechanism how PCSK9 mediates LDLR internalization and degradation has not yet been elucidated. Interestingly, the fully folded C-terminal Cysteine-histidine rich domain (CHRD) structure of PCSK9 has a distinct structural similarity to the resistin homotrimer. CHRD of PCSK9 does not interact directly with the LDL receptor, but the CHRD is nevertheless required for PCSK9 mediated LDLR degradation. Previously, we identified adenylyl cyclase-associated protein 1 (CAP1) as a functional receptor for human resistin and clarified its intracellular signaling pathway to modulate inflammatory action of monocytes. We showed PCSK9 directly interacts with CAP1 *in vitro* and *in vivo*. Furthermore, interaction between PCSK9 CHRD and CAP1 SH3 domain is crucial for LDLR degradation. High-fed mice deficient CAP1

(CAP1$^{-/+}$) significantly display decreased low-density lipoprotein cholesterol levels in serum and increased LDLR protein in liver without significant change in its mRNA level. We also found that binding between CAP1 and PCSK9 occurs in lipid-raft on 30 minutes after treatment of PCSK9. Caveolin 1 knockdown in HepG2 cells did not show a decrease in LDLR. In contrast, clathrin knockdown cells caused the degradation of LDLR in a treatment of PCSK9 dose-dependent manner. Taken together, we suggested that PCSK9/CAP1 axis stimulates LDLR internalization for degradation in caveolae lipid raft dependent pathway, distinct from clathrin-dependent pathway for LDLR recycling.

Methods: In this study, we analyzed that CAP1 dependent PCSK9-LDLR degradation, endocytosis mechanism in transient CAP1 knockdown human hepatic cells (HepG2) and TALEN-mediated CAP1$^{-/+}$ mouse.

Results: CAP1-SH3 domain binds to PCSK9 directly. CAP1-PCSK9 complex increased LDLR degradation through lysosomal pathway. CAP1 targeting siRNA in HepG2 cells resulted in abolished LDLR degradation. These pathways are mainly showed caveolin 1 rich lipid-raft. Although caveolin 1

knockdown HepG2 cells abolished LDLR degradation treated PCSK9. In addition, lipoprofile analysis in CAP1$^{-/+}$ mouse showed that LDL cholesterol physiological level in high-fed mice was decreased than wild type mice. Supportive results were obtained with an *in vitro, in vivo* system.

Conclusions: The sorting of PCSK9 to the CAP1-LDLR is required for caveolae lipid raft to promote lysosomal LDLR degradation. This study provides valuable insights into mechanism regulating cholesterol homeostasis and LDLR degradation.

Keywords; Adenylyl cyclase associated protein-1, Low density lipoprotein receptor, Proprotein convertase subtilisin/kexin type-9, Caveolin1, Endocytosis.

Student number; 2009-31343

CONTENTS

LIST OF FIGURES

LIST OF ABBREVIATIONS

CAP1: Adenylyl cyclase associated protein 1

SH3 domain: Proline rich SH3 binding domain

rhResistin: recombinant human resistin protein

CAV1: Caveolin 1

PCSK9: Proprotein convertase subtilisin/kexin type 9

CHRD: Cystein-histidine-rich domain

LDL receptor: Low-density lipoprotein receptor

LDL-c: Low-density lipoprotein-cholesterol

LAMP2: Lysosomal associated membrane protein 2

EEA1: Early endosome antigen 1

INTRODUCTION

Elevated plasma levels of LDL-cholesterol (LDL-C) are a cardinal risk factor for coronary heart disease. LDL particles are formed in the circulation as a catabolic product of triglyceride-rich lipoprotein metabolism and are removed by LDL receptor (LDLR)-mediated endocytosis in the liver. Circulating levels of LDL are delicately sensitive to changes in LDLR activity (1). LDLR activity is controlled at the transcriptional level by feedback inhibition and at the post-translational level by targeted degradation through the action of proprotein convertase subtilisin/kexin type 9 (PCSK9) (2-5). LDLR comprises a large extracellular domain with seven ligand-binding repeats, three EGF repeat domains (EGF-A, EGF-B and EGF-C), an *O*-linked sugar domain, and an YWTD domain (5). Following internalization, LDLR undergoes a conformational change upon exposure to the endosomes that releases bound LDL particle. LDL particle is trafficked to lysosomes, whereas the receptor itself is recycled back to the cell surface (6). PCSK9 is a soluble protein that is secreted primarily from hepatic cells and that directly regulates serum

LDL levels by targeting LDLR for lysosomal degradation (7, 8). In the endoplasmic reticulum, PCSK9 is auto-catalytically cleaved, releasing its prodomain. The prodomain then reattaches near the catalytic domain and forces PCSK9 into an auto-inhibitory conformation that lacks detectable protease activity (9). After PCSK9 binds to LDLR on the cell surface, the complex is internalized, and their interaction tightens as along the lysosomal route by which PCSK9 mediates LDLR degradation (10-13). However, when bound to PCSK9, LDLR is internalized and escorted to lysosomes for degradation through unknown mechanism (14). Interestingly, the catalytic domain of PCSK9 binds with LDLR and the other part of PCSK9, or Cystein-histidine-rich domain (CHRD) is suspected to interact with a putative membrane-bound protein that escort the protein complex toward lysosomal degradation (10). Recently, the CHRD of PCSK9 has been reported to have structural homology with the human resistin C-terminal domain homotrimer (26) a proinflammatory cytokine expressed in monocytes and macrophages to induced atherosclerosis (15). In our previous report, we identified adenylyl cyclase-associated protein 1 (CAP1), a highly-conserved actin-binding protein

first isolated as a component of the *Saccharomyces cerevisiae* adenylyl cyclase complex (20, 21), as a surface receptor for human resistin binding its C-terminal domain homotrimer (22). Since CAP1 was known to regulate actin filament dynamics to be important for cell morphology, migration, and endocytosis (22), we hypothesized that CAP1 is the unknown protein that interact with CHRD of PCSK9 to escort LDLR-PCSK9 complex toward lysosomal degradation. Plasma membrane is internalized by clathrin-dependent and independent way (19). LDLR degradation has been known for clathrin-mediated endocytosis, which targets proteins to the early endosome and goes to the ubiquitin-dependent sorting processes. However, the mechanism by which PCSK9 binding at the cell surface targets the LDLR for degradation is not understood. LDLR degradation mediated by PCSK9 is not protected in the hypertonic media implying the existence of clathrin-independent pathway. Lipid rafts are cholesterol- and sphingolipid-rich domains in the membrane, and able to form membrane invaginations called caveolae that are rich in caveolin 1 protein (21). Caveolae dependent endocytosis functions in controlling receptor down regulation as well as internalization of toxins, SV40 virus and

glycosyl phosphatidylinositol (GPI)-anchored proteins. Here we show that LDLRs are internalized by both clathrin- and caveolae lipid raft dependent pathways (21-24). We demonstrate that although receptor internalization into the EEA1 positive compartment both through clathrin-mediated and through caveolae lipid raft mediated pathway, LDLR degradation is dependent on caveolae lipid raft pathways. Thus, binding PCSK9 and CAP1 during LDLR endocytosis determined LDLR destiny to the degradation from recycling.

MATERIALS AND METHODS

1. Animals and CAP1$^{-/+}$ KO mice generation

CAP1$^{-/+}$ KO mice were created using a pair of transcription activator-like effector nucleases (TALENs) from Life Technologies targeting exon 3 of mouse CAP1. TALEN binding sites are underlined below with a 15 base pair spacer between the 2 sites.

CAP1 exon3 TALEN R

5'-TCCCGTGGCAGAGTACTTGAA - 3'

3'-TCTGCACATCTCCCCCGATC – 5'

CAP1 exon3 TALEN L

5' – TGAAGATGAGTAAGGAGAT -3'

3' - TGTCCTTACGTGTTTCTGC – 5'

Design, cloning and validation of the TALENs were performed by ToolGen-Genomics Toolmaker. Messenger RNA (provided from Life Technologies) for each of the TALENs were diluted in RNase free microinjection buffer to a final concentration of 4.0ng/㎕ for each TALEN (8.0 ng/㎕ total concentration). The TALENs were microinjected into the pronucleus of fertilized one-cell embryos (0.5 days post coitus) obtained from the mating of C57BL/6 males to super-ovulated C57BL/6 female

mice. Microinjected eggs were transferred to pseudopregnant Swiss Webster recipients. Founder pups were screened for TALEN induced mutations in CAP1 by sequencing across exon 3. Two founders, one with a 5 bp deletion and the other with a 29 bp deletion were expanded for further analysis.

Age-matched (8- to 12-week-old) male CAP1$^{-/+}$ knockout mice and CAP1$^{+/+}$ littermates were used as controls (WT). Starting at 8 weeks of age, mice were randomized into different groups, which were fed with the two types of diets. For the control mice and CAP1$^{-/+}$ knockout mice, the animals were fed with either HFD (D12451; 60% fat by kcal; Research Diet Inc. New Brunswick, NJ, USA) or standard rodent chow diet (AIN-93M; Research Diet) Animal sample size for each individual study was chosen based on literature documentation of similar well-characterized assays. Afterwards were sacrificed under isoflurane anesthesia. Tissues were rapidly taken, freshly frozen in liquid nitrogen, and stored at −80°C until needed for immunoblot analysis. Other parts of tissues were fixed for histological and immunohistochemical analysis. The animal studies were not blinded to investigators. All animal experiments were performed after receiving approval from the

Institutional Animal Care and Use Committee (IACUC) of Seoul National University Hospital Biomedical Research Institute, Korea.

2. Genomic DNA preparation and PCR genotyping

Genomic DNA was prepared from liver, BAT and spleen using DNeasy blood and tissue kit (Qiagen, Valencia, CA, USA) following manufacturer's instruction. PCR were carried out using the primers

Fwd; 5' - CTCTCTAAGTGATTGGGACAA - 3'
Rev; 3' - AAGACTGCCAGGACCTTCTCCA - 5'.

3. Cell culture and Treatment

Human HepG2 hepatocytes, human embryonic kidney 293 cells (HEK293T) and TALEN mediated hCAP1 knock-out 293T were cultured in DMEM (Invitrogen Life Technologies, Carlsbad, CA, USA) supplemented with 10% (v/v) FBS (GIBCO, Grand Island, NY, USA), 100 unit ml-1 of penicillin (Invitrogen Life Technologies, Carlsbad, CA, USA), 100 μg ml-1 of streptomycin (Invitrogen Life Technologies, Carlsbad, CA, USA) at 37℃ and 5% CO_2. For LDL receptor degradation assay, cells were switched into DMEM without FBS for at least 4 h prior to assay. 2 μg/ml rhPCSK9-His (PeproTech Inc.Rocky Hill, NJ,

USA) was then added directly to the culturing medium. In some experiments, cells were co-treated with 10μM Lactacystin (Cayman Chemical, Ann Arbor), 100nM E-64d (Cayman Chemical, Ann Arbor, USA), 200nM Bafilomycin (Cayman Chemical, Ann Arbor, USA), vehicle(Dimethyl sulfoxide)(Cayman Chemical, Ann Arbor, USA) along with 2μg/ml rhPCSK9 for 4hr at 37℃.

4. RNA interference and Transfection

For knockdown of CAP1 siRNA and Caveolin1 siRNA molecules was synthesized by QIAGEN. The CAP1 target sequence was 5'-AAACCGAGTCCTCAAAGAGTA-3'. The Caveolin1 target sequence was 5'-AAAAGAGCTTCCTGATTGAGATT-3'. For knockdown of molecule was synthesized by as a control, negative control siRNA (non-silencing siRNA) was purchase from QIGEN. The Clathrin heavy chain siRNA were obtained ON-TARGETplus SMARTpool by Dharmacon,Inc. For target knockdown, siRNA oligos were transfected using RNAiMax Lipofectamine (Invitrogen Life Technologies, Carlsbad, CA, USA) according to the manufacturer' s instructions.

5. Real-time quantitative PCR analysis

Determination of tissue mRNA by RT-qPCR, all the tissues were frozen in liquid nitrogen and stored at 80℃ until analysis. Total RNA was prepared from WT, CAP1 +/- knockout mouse liver (0.4 g). Briefly, tissues were homogenized with a TRIzol Reagent (Invitrogen Life Technologies, Carlsbad, CA, USA) by centrifugal force (30,000 rpm for 1 min). Tissue homogenates were supplemented with 0.2 volumes of chloroform, mixed thoroughly and centrifuged at 12,000 rpm for 15 min. Supernatant were supplemented with 1 volume of 70% ethanol mixed thoroughly and transferred to column for RNA purification. Up to 1 μg of RNA was converted into cDNA according to the PrimeScript™ 1st strand cDNA Synthesis Kit (Takara Bio, Otsu, Japan). Real-time PCR was performed using the SYBR Green PCR Master Mix (Roche Applied Science, Indianapolis, IN, USA) with specific primers. Real-time samples were run on an ABI PRISM-7500 sequence detection system (Applied Biosystems). Relative quantification of gene expression was calculated using the 2-⊿⊿Ct method using 18srRNA as reference. The following primers were used:

CAP1-Fwd; 5'-ATTCTCTCTCCGGT-3'

Rev; 5'-TAAGAGTTCCGCCTCACCTC-3'

LDL receptor-Fwd; 5'-TGGCCCCAAGTTCAAGT-3'
Rev; 5'-ACAGGCACTCAGAGCCAATC-3'

ApoB- Fwd; 5'-CAGCCAATAATGTGAGCCCCT-3'
Rev; 5'-TCATCTTGAGTTCAGGCTGCTT-3'

PCSK9- Fwd; 5'- GTGACCCTGCCCTCAATCTC-3'
Rev; 5'- TTTGTCTTCGCCCAGAGCAT-3'

6. Protein extraction and Immunoblotting

Cells or tissues were collected and homogenized within lysis buffer containing 10 mM Tris-HCl (pH 7.9), 10% glycerol, 0.1 mM EDTA, 100 mM KCl, 0.2% NP-40, 0.5 mM PMSF, 1 mM dithiothreitol (DTT), Haltprotease & Phosphatase inhibitor cocktail mini-complete protease inhibitor cocktail (Thermo Fisher Scientific, San Jose, CA, USA) if required. Nuclei and insoluble debris were pelleted in an eppendorf microcentrifuge at 10,000 rpm for 5 min at 4 ℃. Cell extracts were then stored at -20 ℃ or immediately subjected to SDS-PAGE. For SDS-PAGE, cell extracts were mixed with 5× loading buffer and heated at 95 ℃ for 5 min before electrophoresis. For immunoblotting, proteins were transferred to polyvinylidene difluoride (PVDF) membranes (Millipore, IPVH00010,

Billerica, MA, USA). Prior to incubating with primary antibody, membranes were blocked with 5% skim-milk in PBS supplemented with 0.1% (v/v) Tween-20 for 1 h at room temperature. Chemiluminescent detection was completed with enhanced chemiluminescent (ECL) western blotting reagents (Amersham Biosciences, Rosendaal, The Netherlands, UK).

7. Antibodies for Western analysis

Primary antibodies used in this study were as follows: anti-CAP1 antibody (Santa Cruz Biotechnology, CA, USA, sc-100917, sc-137637), anti-PCSK9 (Cell Signaling Technology, Beverly, MA, USA #85813), anti-LDL receptor (Abcam, Cambridge, MA, USA, ab52818), anti-Caveolin1 (Santa Cruz Biotechnology, CA, USA, sc-894), anti-Clathrin HC (Santa Cruz Biotechnology, CA, USA, sc-58714), anti-EEA1(Santa Cruz Biotechnology, CA, USA, sc-6415), anti- Flag (Cell Signaling Technology, Beverly, MA, USA #14793), anti-His tag (Cell Signaling Technology, Beverly, MA, USA, # 2365), anti-mFc-HRP (Sigma Aldrich, St. Louis, MO, USA, A0168), anti-GAPDH (Sigma Aldrich, St. Louis, MO, USA, SAB2100894). As secondary antibody, anti-mouse IgG HRP (Promega, Madison, WI, USA), anti-goat IgG HRP (Promega,

Madison, WI, USA) or anti-rabbit IgG HRP (Promega, Madison, WI, USA) were used. ECL or ECL-PLUS (Amersham Biosciences, Rosendaal, The Netherlands, UK) was used for detection.

8. Immunoprecipitation

To identify CAP1 and PCSK9 interaction on Liver tissue, total lysates from $CAP1^{+/+}$ and $CAP1^{-/+}$ knockout mouse livers were incubated for 1hr at 4℃ with anti-CAP1 antibody (Santa Cruz Biotechnology, CA, USA, sc-100917), anti-PCSK9 (Cell Signaling Technology, Beverly, MA, USA #85813), or normal mouse IgG (Santa Cruz Biotechnology, CA, USA, sc-2025), normal rabbit IgG (Santa Cruz Biotechnology, CA, USA, sc-2027). After incubation with the antibody, the lysates were incubated with protein A/G agrose beads (Santa Cruz Biotechnology, CA, USA, sc-2003) for 2hr at 4℃. After washing the beads were resuspended in 2X reducing sample buffer and heated for 5min at 95℃ to dissociate captured antigen from beads. Beads were removed by centrifugation at 2,500rpm and immunoprecipitates from supernatants were separated on a 10% SDS-PAGE Tris-Glycine gel and transferred to a PVDF membrane. The PVDF membrane was

washed and blocked with 5% fat-free milk. Following washing, the membrane was incubated with primary antibodies.

9. *In Vitro* Binding Assay by IP/Western

TALEN mediated CAP1 knockout HEK 293 cells were transfected with his tagged constructs to wtPCSK9-Flag by Park (24) and C-terminal of wild type CAP1-mFc and only SH3 domain of CAP1-His. The whole cell lysates were harvested with a lysis buffer and immunoprecipitated using anti-mFC tag antibody (Cell Signaling, #2365) with bead (Santa Cruz Biotechnology, CA, USA, ImmunoCruz IP/WB Optima C System, sc-45040). After washing with PBS, the immunoprecipitated sample was incubated with rhPCSK9 in binding buffer (20mM Tris-HCl, pH7.4, 200mM NaCl and 1mM MgCl2), resuspended with 2X reducing electrophoresis buffer and boiled at 95-100℃ for 5 minutes to denature the protein and separate it from the protein-IP matrix. The proteins were separated by SDS-PAGE and transferred to PVDF membrane. The interaction between human CAP1 and PCSK9 was detected with anti-Flag, mFC tag antibodies.

10. Direct Binding Assay: Surface Plasmon Resonance

The protocol of surface plasmon resonance spectroscopy (SPR) in this study of real-time direct binding of hPCSK9 and hCAP1 was performed by using a Biacore X100 (Reichert Technologies, Depew, New York, USA). The Sensor Chip CM5 with pre-immobilized hPCSK9 (2mg/ml) in one flow cell was first saturated with hPCSK9 protein. To analyze the binding kinetics, various concentrations of hCAP1 diluted in HBS-EP buffer (consisting of 0.01 M HEPES [pH7.4], 0.15 M NaCl, 3 mM EDTA, 0.005% Surfactant P20) were injected onto the sensor chip for 120 s at 30 ml/min, and the response unit (RU) was then recorded. After injection of the analytes was stopped, HBS-EP buffer was poured over the chip for 130 s at 30 ml/min to allow the bound analytes to dissociate from the immobilized hPCSK9, and dissociation curves were obtained. The RU elicited by injecting HBS-EP buffer was used as the vehicle control. Biacore X100 control software was used to measure the changes in RU and to plot the binding curve. The curves obtained from the SPR experiments were analyzed, and the dissociation equilibrium constant (KD) of hCAP1 to immobilized hPCSK9 was calculated using kinetic evaluation

software. The dissociation equilibrium constant KD (M) was derived from the equation, KD = kd/ka, where kd and ka are dissociation- and association-rate constants, respectively.

11. Isolation of membrane raft and cytosolic fraction

Membrane raft and cytosol were isolated as described previously with slight modifications (Biotechniques.2010; 49: 837-8). Briefly, 5.0×10^5 HepG2 cells per 100mm dish were seeded and treated with 2 μg/ml of rhPCSK9 (PeproTech Inc. Rocky Hill, NJ, USA) for 0min, 30min, 60min in the presence of DMEM media (Invitrogen Life Technologies, Carlsbad, CA, USA). After, cells were harvested, washed two times with ice-cold PBS and treated with 2 mM of DTSSP (Thermo Fisher Scientific, San Jose, CA, USA) for 2 hour at 4℃ with gentle rotation. Then, cells were collected, and pellet was incubated at -80℃ for overnight. Pellets were then lysed in 200 μl of 0.1% Triton X-100 membrane raft isolation lysis buffer (50 mM Tris-HCl [pH7.4], 150 mM NaCl, 5 mM EDTA, 0.1% Triton X-100, 1X protease inhibitor cocktail) using automatic pipet and vortexer for 10 seconds. Total cell lysates were forced through a 23-gauge needle using 5-ml syringe for 20 times on ice and then centrifuged for 20 min at 100x g at 4℃. After, 500 ul of

post nuclear supernatants was adjusted to 40% OptiPrep (Sigma Aldrich, St. Louis, MO, USA) by adding 1 ml of 60% OptiPrep and then placed at the bottom of a 5-ml polyallomer ultracentrifuge tube (Beckman Instruments, Fullerton, CA,USA). Subsequently, samples were overlaid in a step-wise carefully with 1.5 ml of 30% and 5% of ice-cold OptiPrep medium diluted in 0.1% Triton X-100 membrane raft isolation buffer and subjected to ultracentrifugation at 132,000x g at 4℃ for 5 hours. After ultracentrifugation, 15 equal fractions (200 ㎕ /fraction) were collected from top of the tube and membrane lipid-raft fraction and non-raft and cytosolic fraction were combined for immunoblotting. All procedures were strictly carried out on ice.

12. Plasma lipoprotein analysis

To analyze the plasma lipoprotein profiles, the pooled together mouse plasma samples were subjected to fast-performance liquid chromatography (FPLC) analysis using a Superose 6 HR10/300 column (GE Healthcare, Piscataway, NJ, USA), 150 ㎕ of pooled plasma was separated using a buffer containing 0.15 mol/L NaCl, 0.01 mol/L Na2HPO4, and 0.1 mmol/L EDTA, pH 7.5, at a flow rate of 0.5 mL/min. Forty 0.5mL fractions

were collected, and all fractions were analyzed for cholesterol levels as previously described (Babaev et al., 2008; Fazio et al., 2002). The high-density lipoprotein (HDL) and very low-density lipoprotein (VLDL)/ low-density lipoprotein (LDL) cholesterol levels were also quantified the HDL and VLDL/LDL Cholesterol Assay Kit (Abcam, Cambridge, MA, USA, ab65390).

13. Histological and Immunohistochemical Analysis

When animals were sacrificed, livers were rapidly fixed in 10% phosphate-buffered formalin acetate at 4℃ overnight and embedded in paraffin wax. Paraffin sections (5 ㎛) were cut and mounted on glass slides. Immunohistochemistry of liver sections was performed as described previously (Zang et al., 2006). Briefly, antigen retrieval was performed; deparaffinized tissue retrieval was performed; deparaffinized tissue sections were treated with 10mmol/L citrate buffer (pH 6.0) in a microwave (2 min at 700W, repeated 3 times). Tissue sections were using a red alkaline blocked with 10% normal goat serum (Vector Laboratories Inc., Burlingame, CA, USA) in phosphate-buffered saline (PBS) for 30 min. Liver sections were incubated with polyclonal antibodies against CAP1 (1:25 dilution), PCSK9 (7.5 μg/ml), or LDL receptor (6 μg/ml) in PBS with 1% BSA

overnight at 4℃ and then incubated for 1 h at room temperature with a biotinylated anti-rabbit or anti-mouse IgG secondary antibody (dilution of 1:200) using the Vectastain ABC kit. Positive immunoreactivity was visualized phosphatase substrate. To ensure the specificity of the staining, liver sections from each mouse were also stained in parallel with a non-immune rabbit or mouse isotype IgG as a negative control. The development of the staining with the immune IgG was stopped before any nonspecific staining could occur with the non-immune IgG. Staining images were captured and digitalized using an Olympus microscope attached to an Olympus digital camera (DP73).

14. Immunofluorescence staining

For *In vitro* experiments, anti- CAP1 antibody (Santa Cruz Biotechnology, CA, USA, sc-100917, sc-137637), anti-PCSK9 (Cell Signaling Technology,Beverly, MA, USA # 85813), anti-LDL receptor (Abcam, Cambridge, MA, USA, ab52818), anti-Caveolin1 (Santa Cruz Biotechnology, CA, USA, sc-894), anti-EEA1 (Santa Cruz Biotechnology, CA, USA, sc-6415), anti-LAMP2 (Abcam, Cambridge, MA, USA, ab25631) staining were performed on HepG2 cells. Anti-goat IgG Alexa Fluor

633 (Invitrogen Life Technologies, Carlsbad, CA, USA) and anti-mouse IgG Alexa Fluor 488, 555, 633 (Invitrogen Life Technologies, Carlsbad, CA, USA), anti-rabbit IgG Alexa Fluor 488, 555, 633 (Invitrogen Life Technologies, Carlsbad, CA, USA) were used as a secondary antibody, respectively. DAPI staining was performed to identify nuclei. Specimens were observed using a confocal microscope (LSM710, Carl Zeiss AG, Oberkochen, Germany).

15. Statistical analysis

The results are expressed as means ± standard deviations (SD). The differences between the groups were compared by the unpaired t-test or one-way analysis of variance (ANOVA). P values ≤ 0.05 were considered statistically significant. All statistical analyses were performed using SPSS 17.0 (SPSS Inc., Chicago, US).

RESULTS

CAP1 directly binds with PCSK9 through interaction between SH3 domain and CRD

To investigate whether CAP1 binds with PCSK9 as our hypothesis, co-immunoprecipitation was done and the result suggested a physical interaction between CAP1 and PCSK9 in HEK293T cells (Fig. 1A). Endogenous LDLR was also co-immunoprecipitated. To address whether their endogenous forms bind together, liver homogenates from C57BL/6 wild-type (WT) mice were immunoprecipitated with anti-CAP1 antibody, immunoblotted with anti-PCSK9 antibody, and vice versa, which confirmed their interaction (Fig 1B). To test whether their interaction is direct, we performed a far western blot (16). Purified mFc-CAP1 or His-PCSK9 was transferred to a nitrocellulose membrane as a prey in non-reducing condition, respectively. The membrane then was blocked and probed with His-PCSK9 or mFc-CAP1, respectively. This approach identified PCSK9 or CAP1 on the spot in the membrane where the prey is located (Fig 1C), demonstrating

that the PCSK9 and CAP1 interact directly. Finally, we performed a direct binding assay using surface plasmon resonance (SPR) based system. The binding curves showed increased response unit (RU) between PCSK9 and CAP1 in a dose dependent manner. The calculated dissociation equilibrium constant (KD) from the dissociation curves was 1.37 μM (Fig 1D). Herein, we predicted the structure of the PCSK9-binding domain using homology modeling (26) with the region of CAP1. Using Discovery Studio 2.5 (Accelrys discovery studio), we were able to visualize the predicted structure of the PCSK9-binding domain and the predicting structures of the CAP1. Then, to predict the structure of the PCSK9-CAP1 complex, we virtually analyzed the surface geometry of the complex using a protein-protein docking simulation and the score function analysis. The molecular structure of CAP1 was previously described the structure of the SH3-binding domain using homology modeling (20). We were able to visualize the predicted structure of the resistin-binding domain and the known structures of the PCSK9 (39). Then, to predict the structure of the PCSK9-CAP1 complex, we virtually analyzed the surface geometry of the complex using a protein-protein

docking simulation and the score function analysis. Using the Pairwise Shape Complementarity function-based docking algorithm, ZDOCK (40, 41), we inferred several 3D binding structures between the PCSK9 and the PCSK9-binding domain of CAP1. Then, we evaluated the binding free energy of each complex using the Poisson-Boltzmann surface area method (42). Figure 1E depicts the structure of the PCSK9-CAP1 binding complex with the lowest binding free energy, which could be the conformation observed in nature. As shown in Figure 1E, Key binding interactions were identified as charge-charge interactions between the negative charged side chain of Asp34B in CAP1-SH3 BD and the positive charged side chain of Arg659, Ly494 in the PCSK9. Also, the additional three hydrogen bonds between the backbone of Pro22B in CAP1-SH3 BD and the side chain of Ser662 in the PCSK9, the backbone of Pro23B in CAP1-SH3 BD and the side chain of Ser642 in the PCSK9, , the backbone of Pro20B in CAP1-SH3 BD and the backbone of Asp660 in the PCSK9 trimer increase the binding affinity. It suggests interaction between PCSK9 and CAP1-SH3 BD.

CAP1 regulates for PCSK9 mediated LDLR degradation

PCSK9 promoted LDLR degradation in human hepatic cells (HepG2) (Fig 2A). Degradation of LDLR in HepG2 cells in response to high PCSK9 concentrations. To further assess the extent of LDLR degradation in HepG2 cells, we incubated cells with rhPCSK9 at high nonphysiological concentrations (0 – 5 μg/ml). Next, we wanted to determine whether CAP1 is required PCSK9 mediated for LDLR degradation by treating HepG2 cells with CAP1 siRNA (20). Although CAP1 siRNA decreased CAP1 expression levels, PCSK9 treatment did not perturb intracellular LDLR degradation contrast to Control siRNA treated cells (Fig 2B). We suggested that CAP1 function is involved in PCSK9 mediated LDLR degradation. To further substantiate these observations, we performed in vitro binding assays between CAP1-SH3 domain and PCSK9 (Flag-wtPCSK9). Figure2C showed that CAP1 SH3 domain is sufficient to interact with PCSK9. Using Flag-wtPCSK9 and mFc-CAP1 SH3 BD overexpressing HEK 293T cells lysate, we performed Fc pull-down assay. These observations confirm that PCSK9-CHRD binds to CAP1 via the SH3 BD and that likely plays a key role in LDLR degradation. When CAP1 was

depleted with CAP1 siRNA, LDLR degradation by exogenous PCSK9 treatment was totally blocked (Fig 2B). To evaluate whether our observation is specific for CAP1 depletion, we recued CAP1 knockout cell line with wtCAP1 or each CAP1 mutants and tested PCSK9 mediated LDLR degradation. Figure 2D describes that wtCAP1 overexpression and actin BD deletion could rescue PCSK9 mediated LDLR degradation. Therefore this result suggested that CAP1 is required for PCSK9 mediated LDLR degradation in vitro and SH3 domain of CAP1 specifically binds with PCSK9 for LDLR degradation

Low cholesterol level in CAP1$^{-/+}$ knock-out mice.

In the present study, to analyze in vivo gene functions we produced TALEN mediated CAP1 knock-out mouse. To target these genes in the mouse genome, we designed and synthesized highly active TALENs specific to exon 3 of CAP1 (CAP1-TALEN; Fig 3A). First, we measured the expression levels of endogenous CAP1 TALEN mediated CAP1 heterogeneous knock-out mouse (CAP1$^{-/+}$ mouse) compared with WT controls (CAP1$^{+/+}$ mouse), since CAP1 homogenous knock-out mouse was lethal. Endogenous PCSK9 was expressed mainly in

brain, lung, liver and spleen. Up to 16 weeks of age, the CAP1$^{-/+}$ mice and those of age- and sex-matched control mice did not differ to phenotype. Histological examination revealed that no noticeable different CAP1$^{-/+}$ mice compared with controls of organs (brain, heart, lung, liver, spleen, kidney, ovary, stomach and intestine (Fig 3B).

To analyze whether CAP1 regulates LDLR degradation and thereby plasma LDL-C levels in vivo, we determined LDLR and PCSK9 expression in liver of CAP1$^{-/+}$ mice and CAP1$^{+/+}$ mice fed chow diet (CD) or high fat diet (HFD). LDLR expression was significantly increased in CAP1$^{-/+}$ mice compared to CAP1$^{+/+}$ mice. However, there was no significant difference in LDLR gene expression (Fig 3D), which suggests that LDLR amount in CAP1$^{-/+}$ mice regulated at protein level. We measured the lipid profiles in CAP1$^{-/+}$ mice and CAP1$^{+/+}$ mice fed either CD or HFD. CAP1$^{-/+}$ mice had lower total cholesterol levels both at CD and HFD and lower LDL cholesterol level at HFD (Fig 3F). There was no significant difference in plasma triglyceride (TG) and HDL cholesterol levels. Then we fractionized plasma lipoproteins by FPLC in CAP1$^{-/+}$ mice and CAP1$^{+/+}$ mice fed HFD, which confirmed marked decrease of

LDL levels in CAP1$^{-/+}$ mice compared to CAP1$^{+/+}$ mice (Fig 3G). Our results altogether suggest that CAP1 depletion prevent degradation of LDLR and CAP1 lacking resulted in a decrease low density lipoprotein which affect cholesterol homeostasis.

PCSK9-mediated lysosomal LDLR degradation requires caveolin1-mediated endocytosis not clathrin-mediated endocytosis

The notion that PCSK9 targets LDLRs for degradation in lysosomes is based on colocalization of PCSK9 and LDL receptors with lysosome markers by fluorescence microscopy (16). However, Maxwell et al (17) reported that inhibition of lysosomal proteases failed to inhibit the degradation of the LDLR in HepG2 cells expressing PCSK9. We insist that LDLR is required for PCSK9-mediated LDLR degradation through Lysosomal pathway. To confirm this suggestion, After 2 μg/ml rhPCSK stimulation, we also examined the effect of pharmacological inhibition on PCSK9-stimulated LDLR degradation; proteasome inhibitor (10 μM Lactacystin), lysosomal inhibitor (100nM E-64d), auto-phagosome inhibitor (200nM Bafilomycin)(Fig 4A). PCSK9-mediated LDLR

degradation was almost completely blocked by the lysosomal protease inhibitor E-64d (Fig 4A). Taken together, these data show that PCSK9-mediated degradation of LDLRs in hepatocytes does not require proteasome, phagosome function but lysosomal degradation. To pursue this hypothesis, PCSK9 conjugated with Cy3 dye (PCSK9-Cy3) was treated to HepG2 and LDLR degradation through lysosomal pathway was determined with PCSK9-Cy3 internalization and lysosomal marker, LAMP2 (Lysosomal associated membrane protein2) at various time points using fluorescence confocal microscopy. After PCSK9-Cy3 treatment LAMP2 had appeared and LDLR decreased (Fig 4B) and PCSK9, LDLR and LAMP2 co-localized (Fig 4D) Whereas EEA1 is not related LDLR lysosomal trafficking and degradation (Fig 4C). Since lysosomal degradation is mediated by early endosome we tested whether early endosome formation in early time point in same method. Figure 4C describes that after PCSK9-Cy3 treatment early endosome marker EEA1 appears only at early time points and localized with LDLR and LAMP2. Since lysosome formation, endosomal trafficking were both blocked by CAP1 depletion, we thought that CAP1 might participate earlier period of LDLR

degradation pathway. Since previous report suggested LDLR is degraded by clathrin mediated pathway not by caveolin1 mediated pathway, to confirm the previous hypothesis, we treated HepG2 cells with caveolin1 or clathrin siRNA tested PCSK9 mediated LDLR degradation (Fig 4E). Unexpectedly, caveolin1 not clathrin was required for LDLR degradation. This result was confirmed by LDLR degradation and LAMP2 formation after PCSK9-cy3 treatment in HepG3 cells (Fig 4F). Together, our results suggest that LDLR degradation occurs through caveolin1 mediated lysosomal degradation and CAP1 might regulate caveolae formation.

The lipid raft-caveolar internalization pathway contains the LDLR-PCSK9-CAP1 complex and is required for LDLR degradation

Previous experiments, we conclude that LDLR interact with PCSK9, CAP1, caveolin1 for endocytosis and LDLR degradation. Next, we assessed the distribution of 4 different molecules and focused on whether they were localized at caveolae or not. That is because one of the critical characteristics is their specific localization. It was reported that caveolin1 were lipid raft-

localizing. Localization to lipid rafts has a crucial meaning in terms of regulatory mechanism of caveolae, which has pivotal roles to regulate signaling components including CAP1 through scaffolding domain of caveolin1 protein. Thus, we examined more precise localization of CAP1 and caveolin1, LDLR, PCSK9 in HepG2 cells. Opti-prep density gradient centrifugation was an efficient method to fractionate lipid raft and non-lipid raft as well as cytosol. By using this method, we readily identified LDLR, CAP1 and caveolin1 localized at lipid raft in rhPCSK9 treated normal HepG2 (Fig 5A). Moreover, we observed that CAP1, caveolin1, LDLR was co-localized after rhPCSK9 treatment for 30min. However, CAP1, caveolin1 depletion in HepG2 cells with rhPCSK9 was not observed 4-molecules recruitment (Fig 5B, C). To evaluate whether CAP1 deficiency affects LDLR degradation through caveolae formation, we also performed as Figure 4D with CAP1 siRNA. We observed decrease in LDLR internalization in HepG2 cell with rhPCSK9 compared with siCAP1 treated cells (Fig 5D). We also remarked that LAMP2 protein level was decreased in CAP1 depleted cells. But, no differences EEA1 expression in CAP1 depleted cells (Fig 5E). Altogether, these data indicate that

caveolin1 is essential for degrading levels of LDLR within the plasma membrane. Since the CAP1 interacting with PCSK9 (Fig 5F), LDLR complex is recruited to the lysosome by caveolin1, we assessed the contribution of the PCSK9-CAP1-caveolin1 complex on LDLR degradation by determining the subcellular co-localization.

a

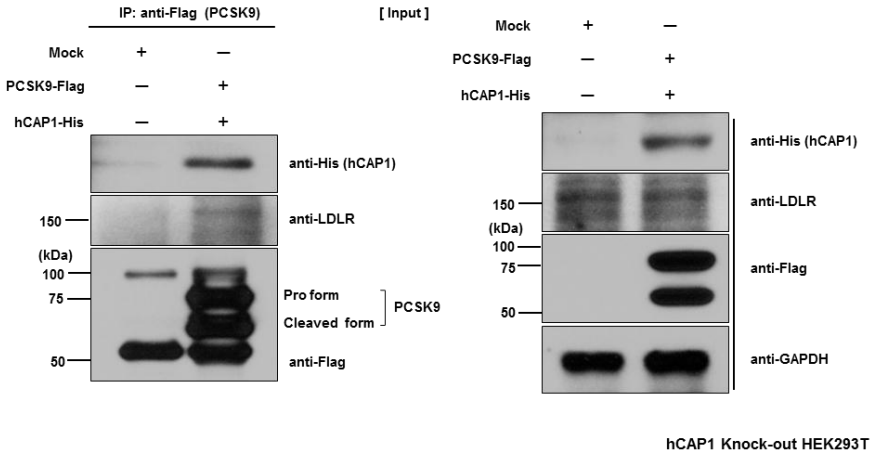
IP: anti-Flag (PCSK9)
Mock + −
PCSK9-Flag − +
hCAP1-His − +
anti-His (hCAP1)
150
anti-LDLR
(kDa)
100
75
50
Pro form
Cleaved form
PCSK9
anti-Flag
[Input]
Mock + −
PCSK9-Flag − +
hCAP1-His − +
anti-His (hCAP1)
150
anti-LDLR
(kDa)
100
75
50
anti-Flag
anti-GAPDH
hCAP1 Knock-out HEK293T

b

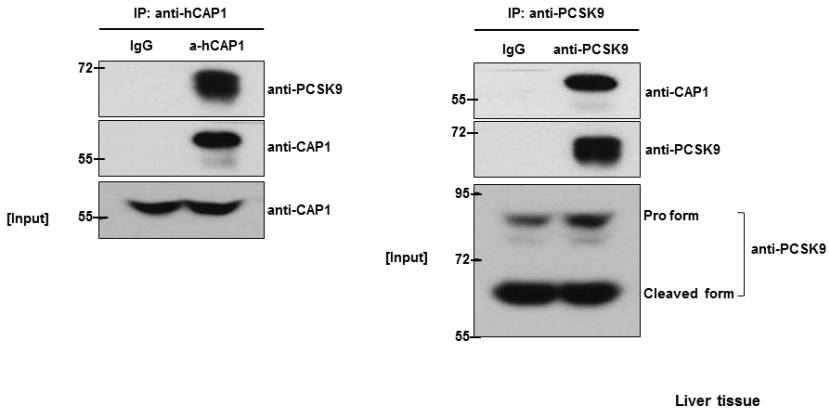
IP: anti-hCAP1
IgG a-hCAP1
72
anti-PCSK9
55
anti-CAP1
[Input]
55
anti-CAP1
IP: anti-PCSK9
IgG anti-PCSK9
55
anti-CAP1
72
anti-PCSK9
95
Pro form
[Input]
72
Cleaved form
anti-PCSK9
55
Liver tissue

c

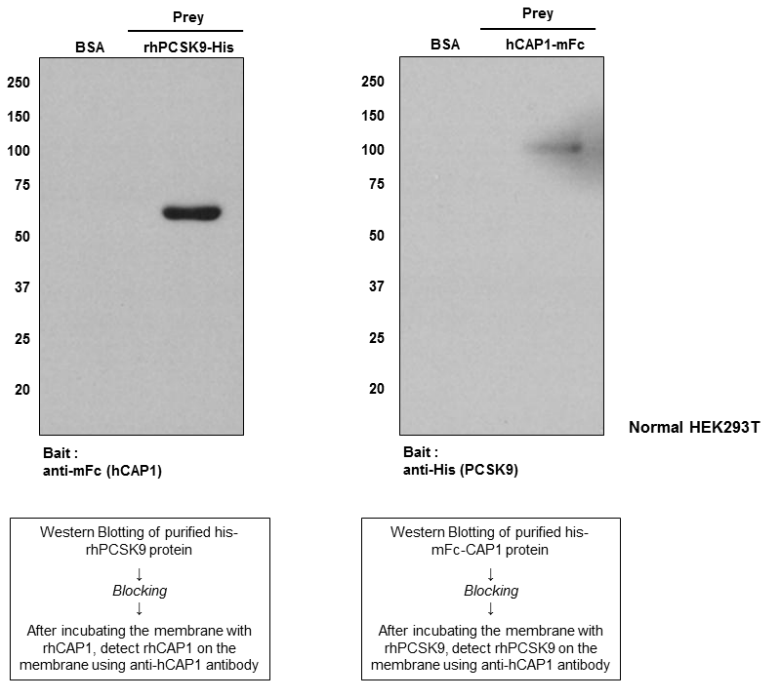
Prey
BSA
rhPCSK9-His
250
150
100
75
50
37
25
20
Bait :
anti-mFc (hCAP1)
Prey
BSA
hCAP1-mFc
250
150
100
75
50
37
25
20
Bait :
anti-His (PCSK9)
Normal HEK293T
Western Blotting of purified his-rhPCSK9 protein
↓
Blocking
↓
After incubating the membrane with rhCAP1, detect rhCAP1 on the membrane using anti-hCAP1 antibody
Western Blotting of purified his-mFc-CAP1 protein
↓
Blocking
↓
After incubating the membrane with rhPCSK9, detect rhPCSK9 on the membrane using anti-hCAP1 antibody

d

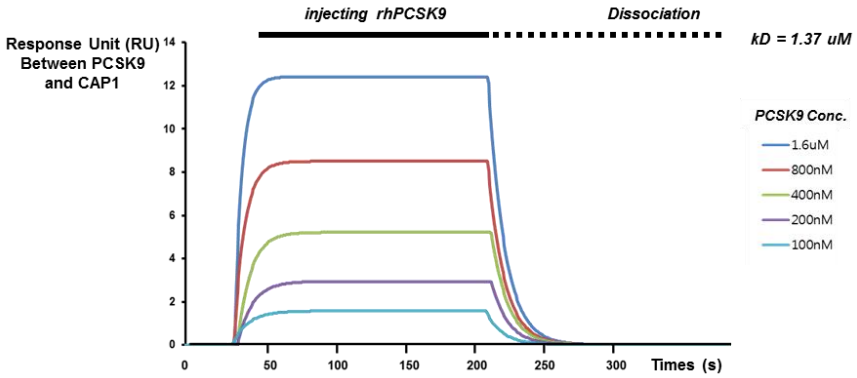
injecting rhPCSK9
Dissociation
kD = 1.37 uM
Response Unit (RU) Between PCSK9 and CAP1
14
12
10
8
6
4
2
0
0
50
100
150
200
250
300
Times (s)
PCSK9 Conc.
1.6uM
800nM
400nM
200nM
100nM

e

3D structure of PCSK9

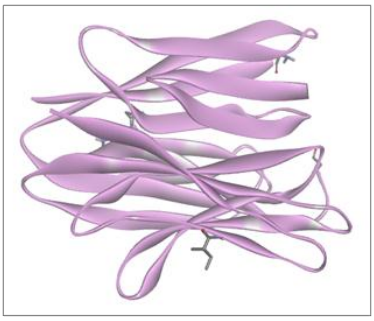

Structural Similarity between PCSK9 and Resistin

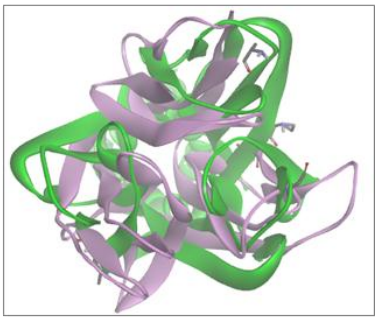

Binding complex of PCSK9 and CAP1-SH3 binding domain

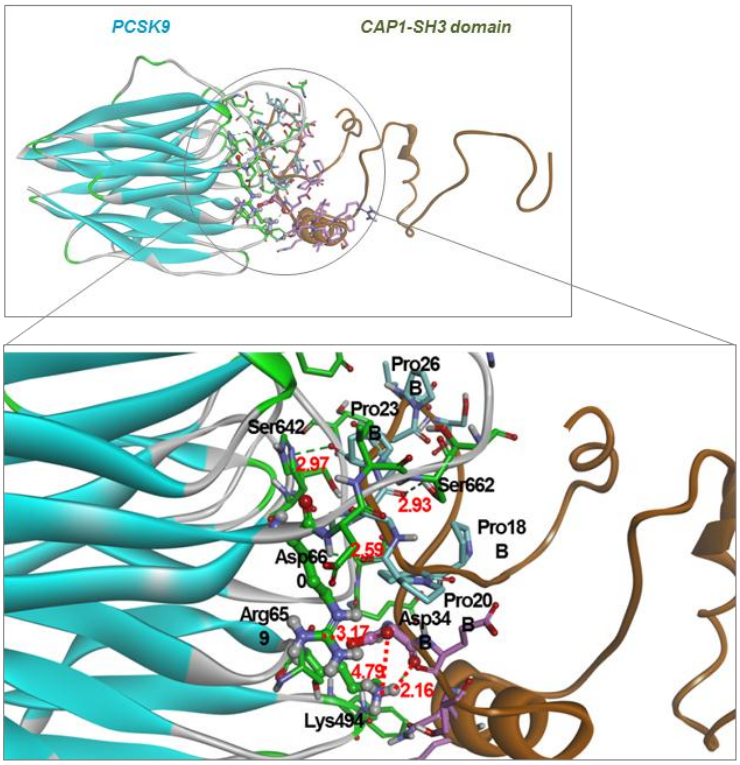

Modeller with Discovery Studio 2.5 (Accelrys Inc.)

Figure1. *In vivo* and *In vitro* PCSK9 Binds Directly to CAP1

(a) CAP1 knock-out HEK293T cells were transfected with constructs expressing Flag-PCSK9 with either His-hCAP1. Interaction with PCSK9 and hCAP1 was detected via co-immunoprecipitation and interaction with endogenous LDLR was detected. (b) Liver lysates of Wild mouse immunoprecipitated for study the endogenous interaction PCSK9 with CAP1. (c) Representative far western blot of mFc-hCAP1 and recombinant rhPCSK9-His. (d) Direct binding assay between rhPCSK9 and CAP1. (e) Predicted secondary structures of the PCSK9-CAP1 SH3 binding domain complex. The PCSK9 is shown as cyan schematic ribbons. The CAP1-SH3 binding domain is shown as a dark brown ribbon. The detailed interactions are illustrated in the magnified black circle.

a

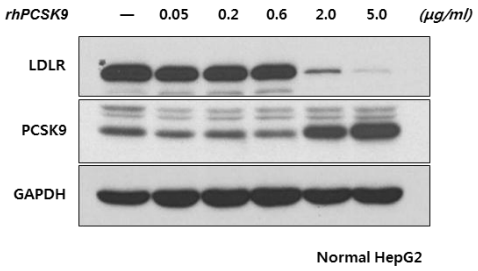
rhPCSK9
—
0.05
0.2
0.6
2.0
5.0
(μg/ml)
LDLR
PCSK9
GAPDH
Normal HepG2

b

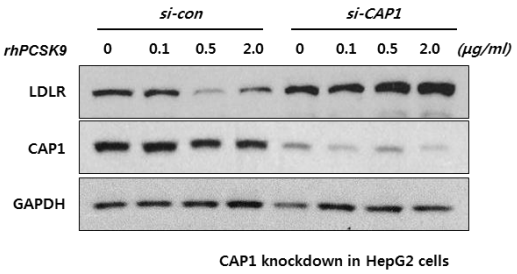
si-con
si-CAP1
rhPCSK9
0
0.1
0.5
2.0
0
0.1
0.5
2.0
(μg/ml)
LDLR
CAP1
GAPDH
CAP1 knockdown in HepG2 cells

c

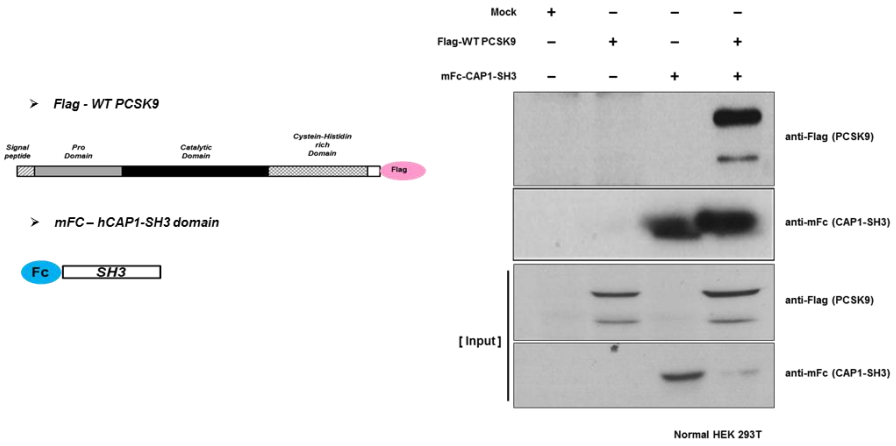
Flag - WT PCSK9
Signal peptide
Pro Domain
Catalytic Domain
Cystein-Histidin rich Domain
Flag
mFC – hCAP1-SH3 domain
Fc
SH3
Mock
Flag-WT PCSK9
mFc-CAP1-SH3
anti-Flag (PCSK9)
anti-mFc (CAP1-SH3)
[Input]
anti-Flag (PCSK9)
anti-mFc (CAP1-SH3)
Normal HEK 293T

d

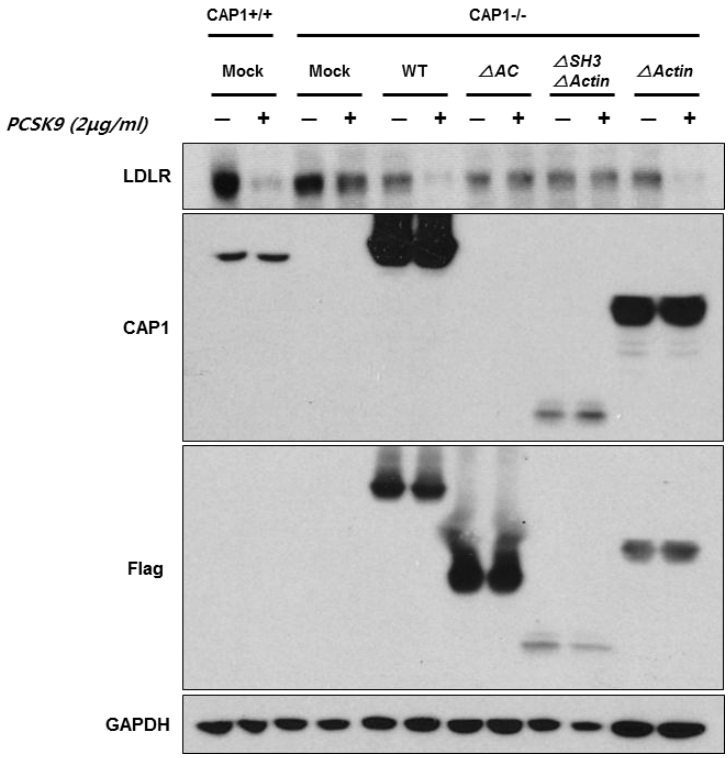
CAP1+/+
CAP1-/-
Mock
Mock
WT
△AC
△SH3
△Actin
△Actin
PCSK9 (2μg/ml)
–
+
–
+
–
+
–
+
–
+
–
+
LDLR
CAP1
Flag
GAPDH

Figure2. CAP 1 mediates the degradation of LDLR in partly by PCSK9.

(a, b) LDL receptor degradation caused by exogenous rhPCSK9 dose-dependently (Vehicle-DMSO, 0.05, 0.2, 0.6, 2, 5 μg/ml) and PCSK9 uptake in HepG2 human hepatic cells. CAP1 levels were reduced using specific small interfering RNAs (siRNAs) in HepG2 cells. siRNA targeting CAP1 abolished PCSK9 induced-degradation LDL receptor. (c) Pull-down assay was performed to study the interaction between Flag-WT PCSK9 and CAP1-SH3 domain using Flag-WT PCSK9 and mFC-SH3 overexpressed in HEK293T cells. (d) CAP1 knockout cell line were transfected with wtCAP1 or each CAP1 mutants and tested 2 μg/ml PCSK9 mediated LDLR degradation.

a

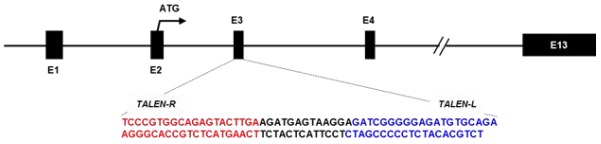

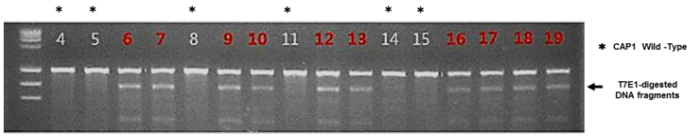

b

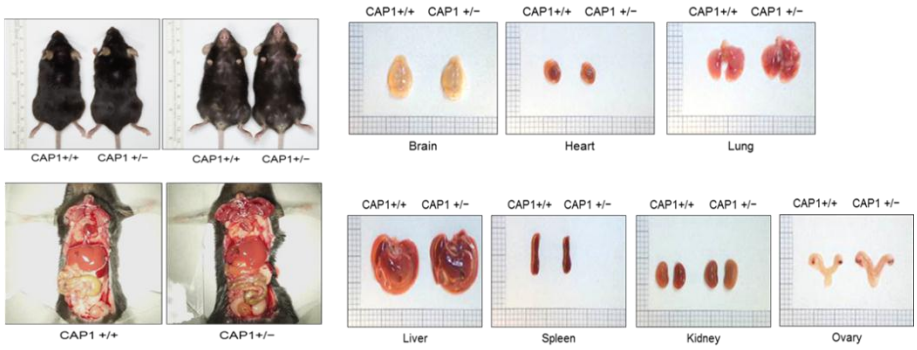

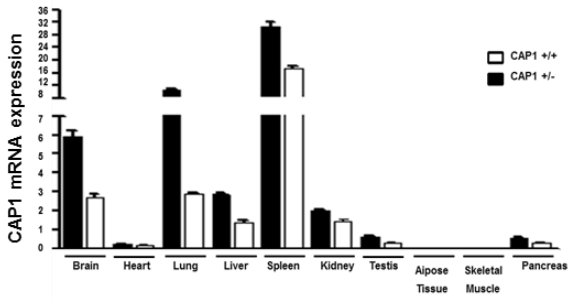

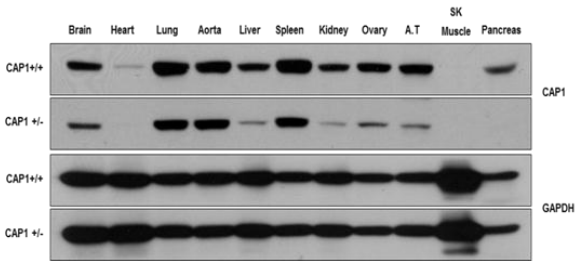

CAP1 protein level in organs

c

➢ **Schematic timeline representing experimental design**

d

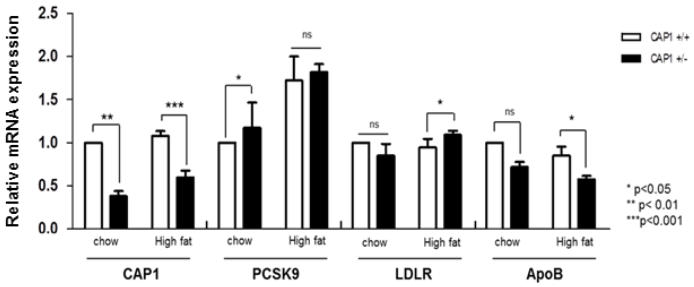

e

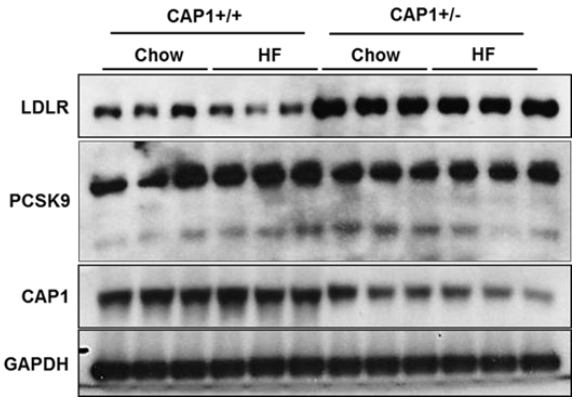

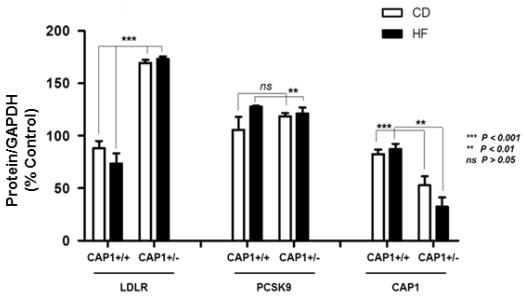

f

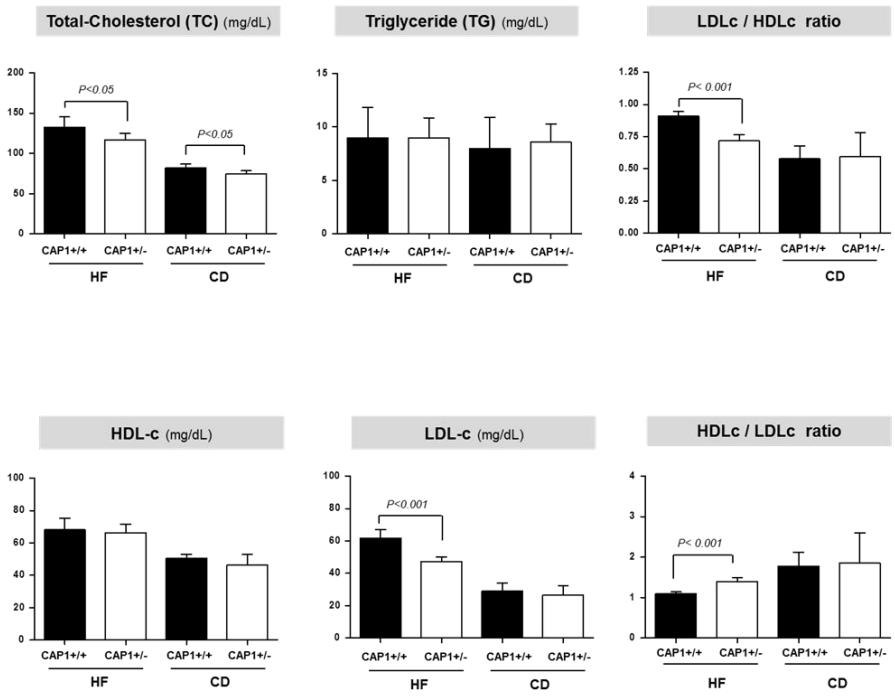
Total-Cholesterol (TC) (mg/dL)
P<0.05
P<0.05
Triglyceride (TG) (mg/dL)
LDLc / HDLc ratio
P< 0.001
HDL-c (mg/dL)
LDL-c (mg/dL)
P<0.001
HDLc / LDLc ratio
P< 0.001
CAP1+/+
CAP1+/-
HF
CD

g

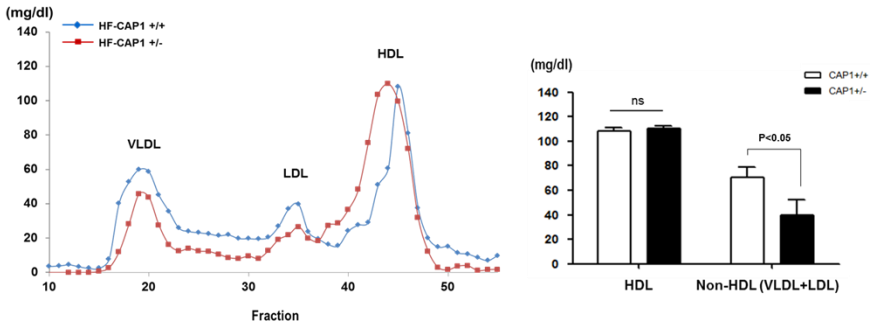
(mg/dl)
HF-CAP1 +/+
HF-CAP1 +/-
VLDL
LDL
HDL
Fraction
(mg/dl)
CAP1+/+
CAP1+/-
ns
P<0.05
HDL
Non-HDL (VLDL+LDL)

Figure3. CAP1 deficient mouse phenotype and Lipid profile.

(a) Cartoon illustrating creation of CAP1 hetero knock-out mouse of TALEN-mediated gene targeting. (b) CAP1 hetero knock-out mouse phenotype. (c) Experimental outline. 8-week-old mice fed with the two types of diets; chow, high-fat diet. (d) qRT-PCR for LDLR, PCSK9 and ApoB in the livers of mice (n = 5 per group, $*p < 0.05$) treated as in C. The error bars represent SD. (e) CAP1, LDLR, PCSK9 protein level in the livers of mice (n = 5 per group) treated as in C. (f) Levels of total cholesterol (TC), LDL-C, HDL-C and triglycerides (TGs) in the plasma of mice (n = 10 mice per group) treated as in E (n = 15 per group). (g) Pooled plasma samples of each experimental group of mice fed the HF diet were separated using FPLC gel filtration. Fifty fractions were collected from each separation. TC content was determined and lipoprotein profile was plotted. (n = 5 per group, $p<0.05$) The error bars represent SD.

a

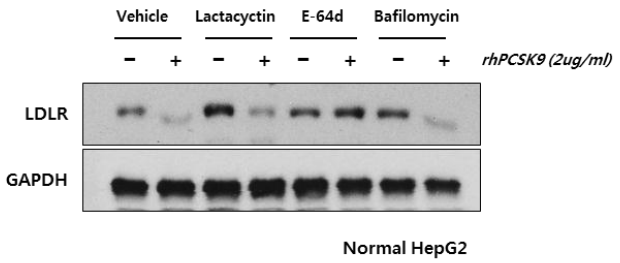
Vehicle
Lactacyctin
E-64d
Bafilomycin
− + − + − + − +
rhPCSK9 (2ug/ml)
LDLR
GAPDH
Normal HepG2

b

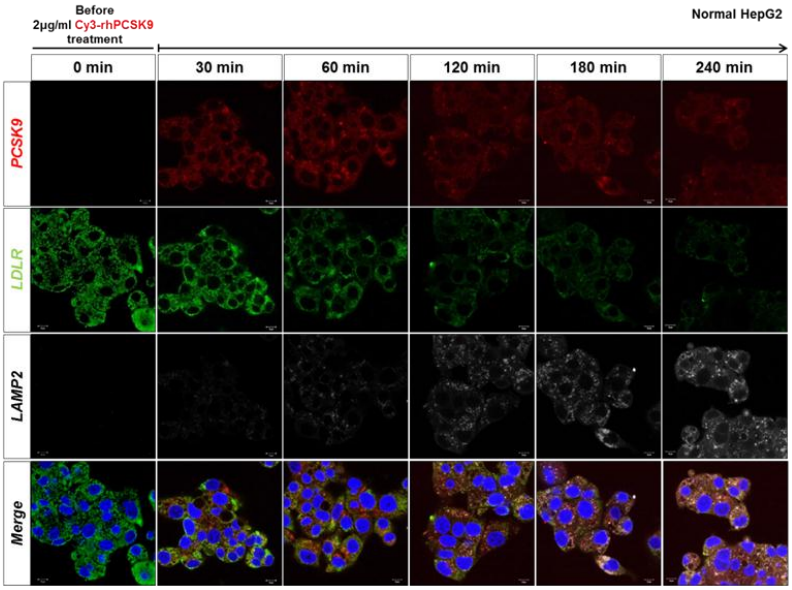
Before
2μg/ml Cy3-rhPCSK9
treatment
Normal HepG2
0 min
30 min
60 min
120 min
180 min
240 min
PCSK9
LDLR
LAMP2
Merge

c

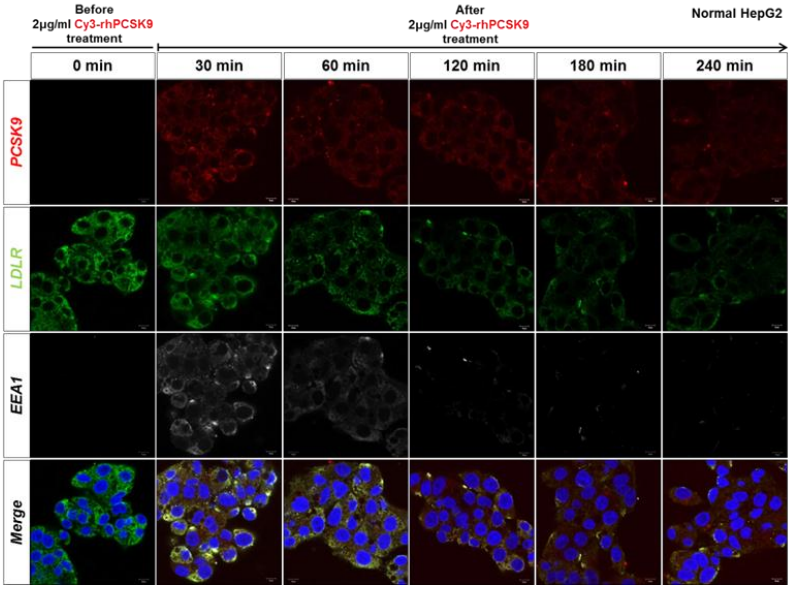
Before
2μg/ml Cy3-rhPCSK9
treatment
After
2μg/ml Cy3-rhPCSK9
treatment
Normal HepG2
0 min
30 min
60 min
120 min
180 min
240 min
PCSK9
LDLR
EEA1
Merge

d

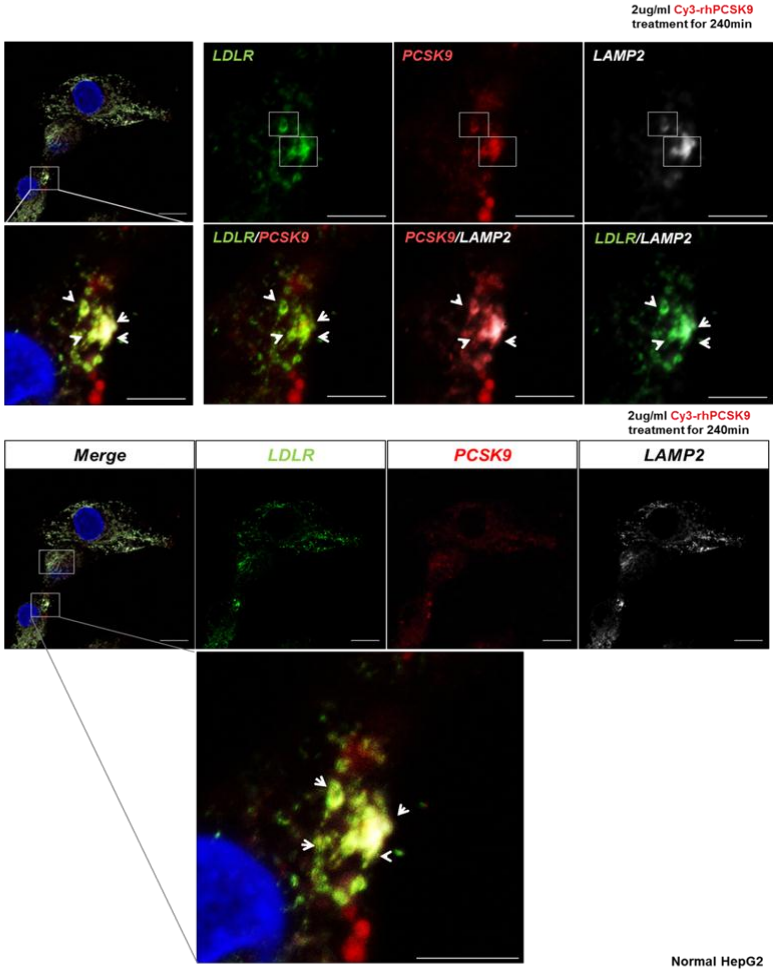
2ug/ml Cy3-rhPCSK9
treatment for 240min
LDLR
PCSK9
LAMP2
LDLR/PCSK9
PCSK9/LAMP2
LDLR/LAMP2
2ug/ml Cy3-rhPCSK9
treatment for 240min
Merge
LDLR
PCSK9
LAMP2
Normal HepG2

e

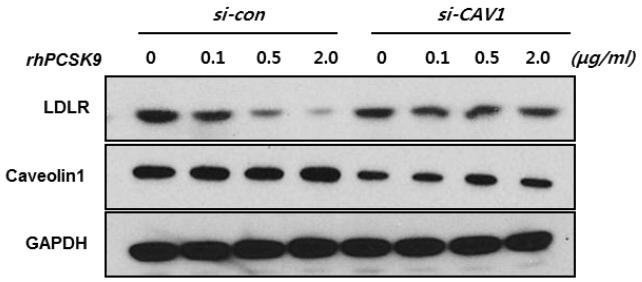

CAV1 knockdown in HepG2 cells

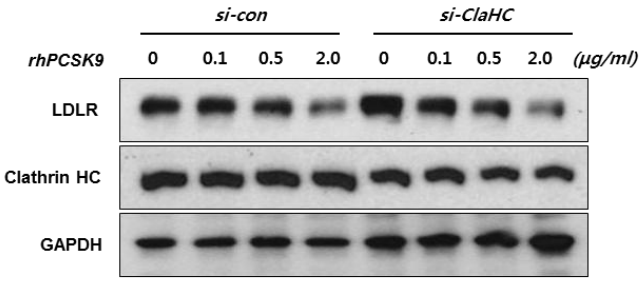

Clathrin HC knockdown in HepG2 cells

f

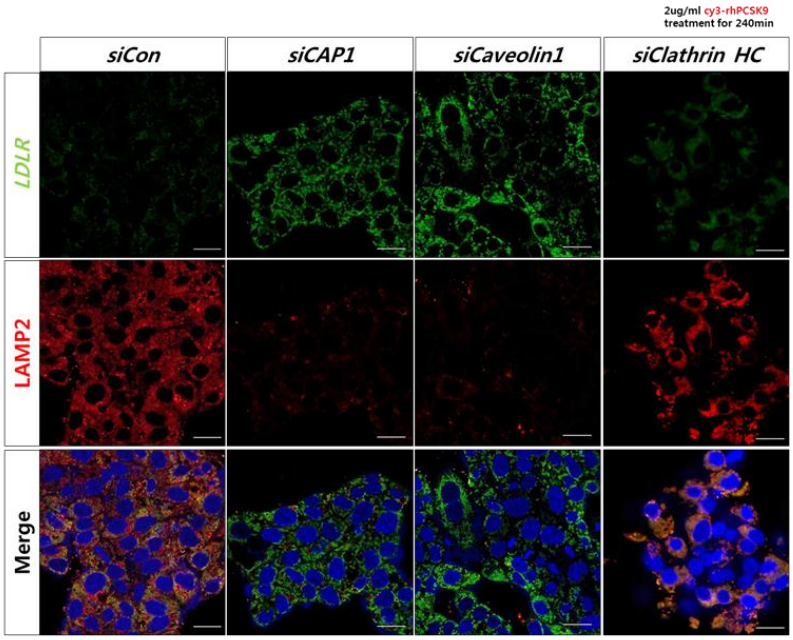

Normal HepG2

Figure4. Caveolin1 is essential for lysosomal degradation of LDLR.

(a) PCSK9-mediated LDLR degradation requires lysosomal pathway. HepG2 cells were treated with proteasome inhibitor; lactacystin (10μM), lysosome inhibitor; E-64d (100nM), auto-phagosome inhibitor; bafilomycin (200nM) along with 2μg/ml rhPCSK9 for 4h. (b, c) Representative confocal images of normal HepG2 incubated with 2μg/ml cy3-rhPCSK9 for time course of LDLR degradation. LDLR (green), LAMP2 (grey), EEA1 (grey) were stained by anti-specific antibodies respectively. Representative image are shown; scale bar, 20μm. (d) LDLR (green) and LAMP2 (grey) staining in HepG2 cells in the absence (upper), or presence of cy3-rhPCSK3 (lower). Colocalization of internalized cy3-rhPCSK9 (red), LDLR (green), LAMP2 (grey) in exogenous cy3-rhPCSK9 treated HepG2 cells examined by immunofluorescence staining. (e) Quantitative western blot data showing levels of LDLR degradation in treating siRNA of caveolin1, clathrin HepG2 cells. (f) Degradation of LDLR and CAP1, caveolin1, clathrin siRNA-CAP1, caveolin1, clathrin treated in HepG2 cells by immunofluorescence staining. Representative images are shown; scale bar, 20μm. LDLR (green) and CAP1, caveolin1, clathrin (red) was stained and imaged by confocal fluorescence microscopy.

a

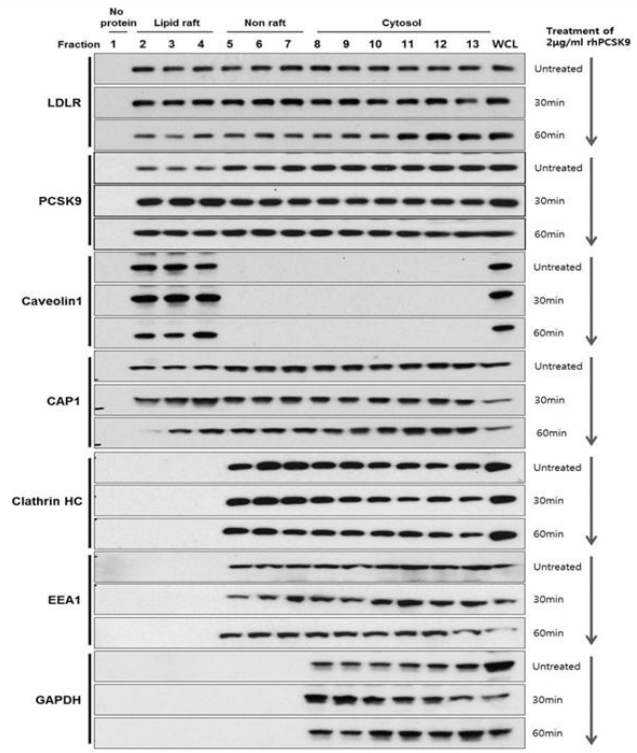
No protein
Lipid raft
Non raft
Cytosol
Fraction 1 2 3 4 5 6 7 8 9 10 11 12 13 WCL
Treatment of 2μg/ml rhPCSK9
LDLR
PCSK9
Caveolin1
CAP1
Clathrin HC
EEA1
GAPDH
Untreated
30min
60min

b

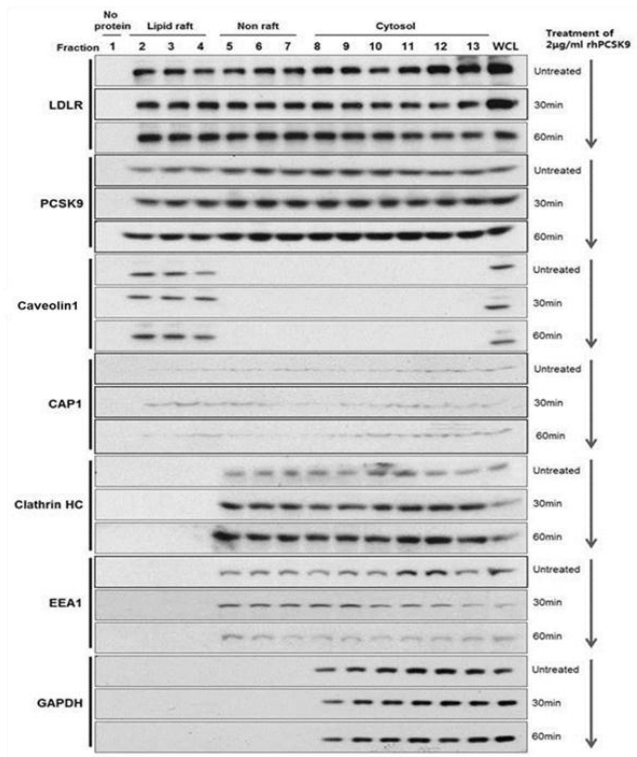
No protein
Lipid raft
Non raft
Cytosol
Fraction 1 2 3 4 5 6 7 8 9 10 11 12 13 WCL
Treatment of 2μg/ml rhPCSK9
LDLR
PCSK9
Caveolin1
CAP1
Clathrin HC
EEA1
GAPDH
Untreated
30min
60min

c

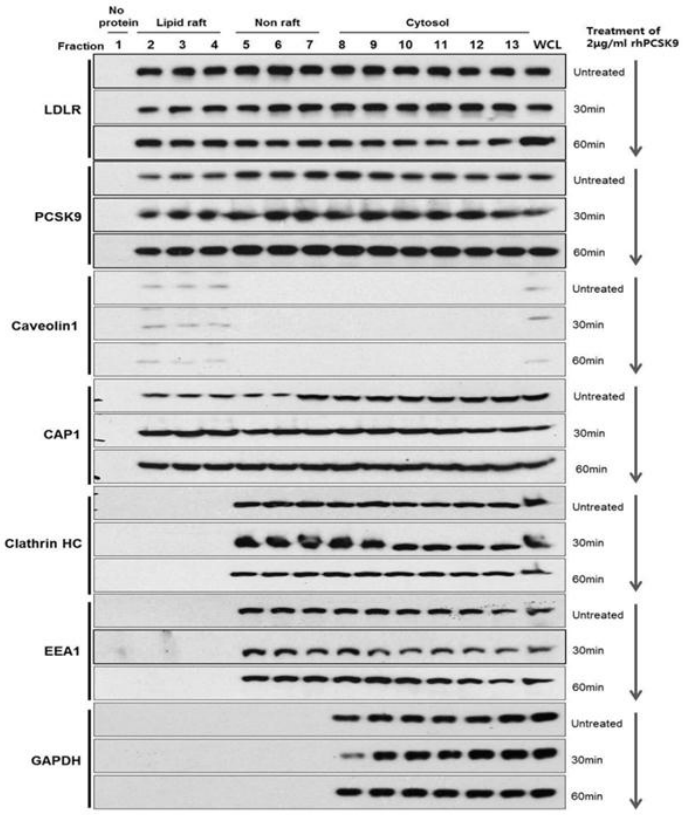
No protein
Lipid raft
Non raft
Cytosol
Fraction 1 2 3 4 5 6 7 8 9 10 11 12 13 WCL
Treatment of 2μg/ml rhPCSK9
LDLR
PCSK9
Caveolin1
CAP1
Clathrin HC
EEA1
GAPDH
Untreated
30min
60min

d

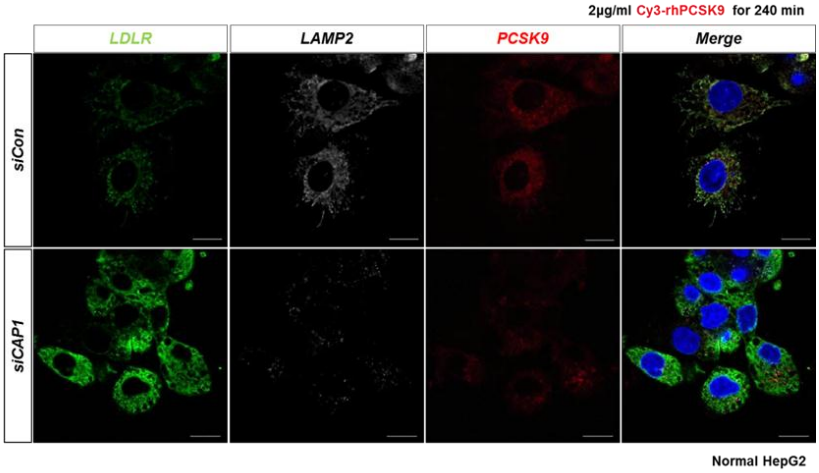
2μg/ml Cy3-rhPCSK9 for 240 min
LDLR
LAMP2
PCSK9
Merge
siCon
siCAP1
Normal HepG2

e

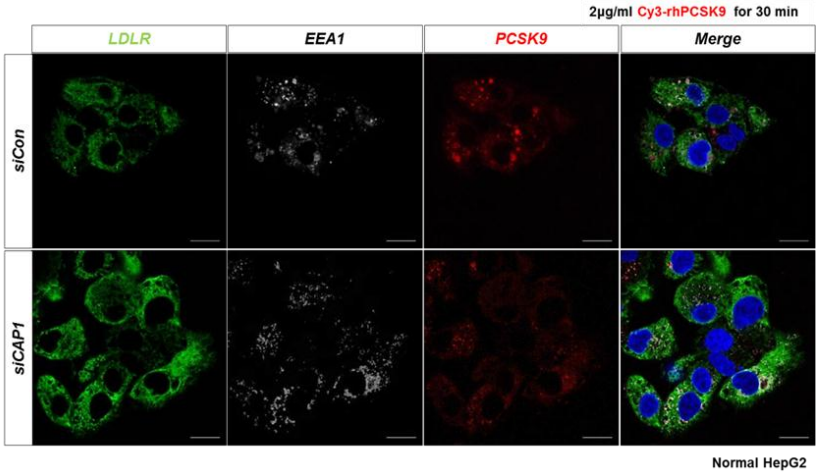
2μg/ml Cy3-rhPCSK9 for 30 min
LDLR
EEA1
PCSK9
Merge
siCon
siCAP1
Normal HepG2

f

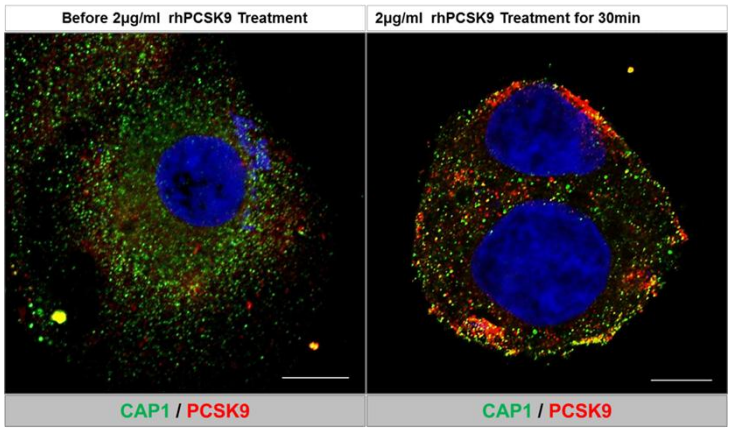
Before 2μg/ml rhPCSK9 Treatment
2μg/ml rhPCSK9 Treatment for 30min
CAP1 / PCSK9
CAP1 / PCSK9

Figure5. LDLR associates with PCSK9 and CAP1 complex localize to lipid-raft. The CAP1, caveolin1 complex is required for lysosomal degradation of LDLR by PCSK9

(a) After treatment of 2μg/ml rhPCSK9 for 30min, 60min in HepG2 cells a localization of LDLR, CAP1, and Caveolin1 was assessed by Opti-prep density gradient ultracentrifugation. (b, c) Treated HepG2 lysate with 2μg/ml rhPCSK9 using siRNA targeting CAP1, Caveolin1 was loaded on an Opti-prep density gradient ultracentrifugation and immunoblotted using antibodies against LDLR, PCSK9, CAP1 and caveolin1. The figure represents results of three independent experiments. (d, e) Representative confocal images of HepG2 using siRNA targeting CAP1 incubated with 2μg/ml cy3-rhPCSK9 for 30min, 240min, LDLR(green), LAMP2 (grey), EEA1 (grey) were stained by anti-specific antibodies respectively. Representative image are shown; scale bar, 20μm. (f) Colocalization of CAP1 and PCSK9 of normal HepG2 incubated with 2μg/ml rhPCSK9 for 30min. CAP1 (green), PCSK9 (red), Representative image are shown; scale bar, 20μm.

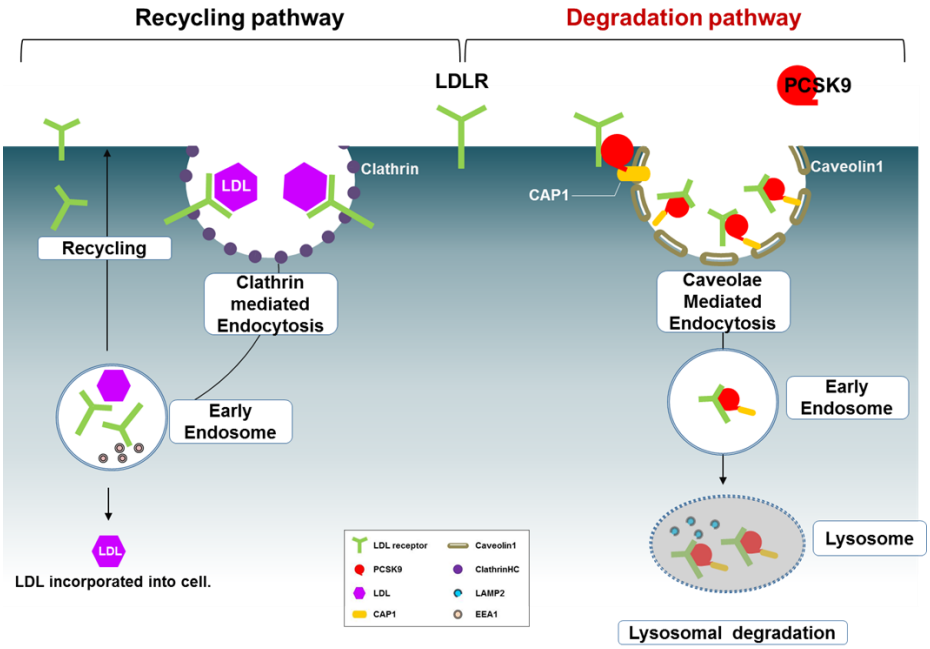

Figure6. Schematic representation of CAP1 mediated lysosomal degradation of LDLR with PCSCK9.

Model for LDLR degradation mediated PCSK9 and CAP1 interaction. Caveolin1-dependent internalization into the lysosome is important for LDLR degradation. The function of this pathway is dictated by the CAP1 and caveolin1.

DISCUSSION

LDLR protein levels are regulated by PCSK9. PCSK9 binds to the extracellular domain of LDLR and induces its internalization in clathrin-coated pits (2). In this study, we showed that PCSK9 employ distinct mechanisms to degrade the LDLR in the lysosome by caveolae mediated internalization. We defined interactions between PCSK9 and LDLR at the plasma membrane that leads to LDLR internalization via a caveolar- and clathrin-independent mechanism. We further showed that LDLR degradation by CAP1 leads to recognition by LDLR-PCSK9 complexs, caveolae formation by caveolin 1, and subsequent lysosomal degradation. We previously identified and engineered a CAP1 that interact with resistin, a small cytokine associated with obesity and diabetes, regulating metabolic and inflammatory disease (20). Surprisingly, the crystal structure of a full-length construct of PCSK9 contains a fully folded C-terminal cysteine-rich domain (CHRD), showing a distinct structural similarity to the resistin homotrimer. This structural relationship between the CHRD of PCSK9 and the resistin family is not observed in primary sequence comparisons and strongly suggests a distant evolutionary link between the two

molecules (26). These results provide important new insights into an evolutionarily conserved pathway for the control of lipoprotein receptor expression and lipid uptake.

Therefore, we hypothesized that PCSK9 and CAP1 would bind and play a crucial role in LDLR degradation. Indeed, Figure 1 indicated PCSK9 effectively interacted CAP1 in mouse liver tissue and in vitro overexpression system vice versa. Also, we performed direct biochemical binding assay as SPR to validate the direct interaction between CAP1 and PCSK9. The binding curves showed increased response unit (RU) between PSK9 and hCAP1 in a dose dependent manner. The calculated dissociation equilibrium constant(KD) from the dissociation curves was 1.37 μM (Fig 2D). An important consideration of this SPR result is high dissociation equilibrium constant, 1.37 μM. Generally, KD >100nM means very weak interaction between proteins. Although, we verified various strong evidences of the direct binding and interaction between hCAP1 and PCSK9 using biochemical binding assays this data has some controversy. It has recently been proposed that the PCSK9 interacts with the LDLR as a secondary step enhancing complex formation at acidic pH on transport to the endosomes

(Yamamoto et al, 2011). We used SPR to show that at neutral pH PCSK9 bound to the CAP1 with a micro-molar dissociation constant. The interaction between PCSK9 and LDLR (wild type and mutants) was also assessed by SPR at acidic pH. In agreement with previous reports (Cunningham et al, 2007; Fisher et al, 2007; Piper et al, 2007), at low pH, the binding affinity was enhanced 50- to 100-fold (KD =8 nM for LDLR wild type). Finally, to overcome low affinity of PCSK9 and CAP1, we tested the protonation of which at low pH might enhance electrostatic attractions in the complex (not shown data).

Interestingly, treatment of PCSK9 could not degrade LDLR in CAP1 deficient cells implying CAP1 has a crucial role in PCSK9 mediated LDLR degradation (Fig 2B). The physical interactions between PCSK9 and CAP1 in living cells have been characterized in detail this study. We showed here that SH3 binding domain of CAP1 actively interact PCSK9 (Fig 2C). Our results predicted CAP1 and PSK9 binding domains that affect degradation of LDLR (Fig 2D).

Furthermore, here we uncover that CAP1 is also critically important in cholesterol homeostasis. We demonstrated this in a

variety of cellular models, and the physiologic importance of our observations has been substantiated in mammalian models (mouse model) of CAP1 deficiency, which display decreased serum LDL cholesterol (Fig 3G). Also, HF−CAP1$^{-/+}$ mice are decreased VLDL, LDL compared with control (Fig 3F). We showed that CAP1 regulates LDLR degradation which suggests that LDLR amount in CAP1$^{-/+}$ mice regulated at protein level. That is, it means that the decrease of LDLR by PCSK9 is suppressed in CAP1$^{-/+}$ mice. Intriguingly, CAP1$^{-/+}$ model indicated large HDL cholesterol levels compared with control (Fig 3G). The capacity of all HDL particles to exert a variety of atheroprotective biological activities, reflecting a wide spectrum of molecular protein, and lipid species present in HDL (Davidson et al., 2009; Heinecke, 2009; Gordon et al., 2010a,b; Camont et al., 2013; Shah et al., 2013). High compositional heterogeneity of HDL directly results in functional heterogeneity among HDL particles, with small, dense, and protein−rich HDL typically displaying potent biological activities (Kontush and Chapman, 2006a; Camont et al., 2011, 2013). Although the relative importance of different biological activities of HDL for atheroprotection remains presently

unclear. Importantly, these findings are significant improvement clue than PCSK9 antagonist therapeutic programs and may provide an alternative avenue. Altogether, this study provides valuable insights in the molecular mechanism of cholesterol homeostasis.

Our study has clarified the pathway for CAP1-mediated target internalization. In higher eukaryotic cells, internalization of plasma membrane proteins and lipids is mediated by clathrin-dependent and independent pathways (28) and after internalization the intracellular itinerary of receptors regulates signal transduction (29-30). Clathrin-mediated endocytosis targets proteins to the early endosome and is an important pathway for downregulating many receptors through ubiquitin-dependent sorting processes involving ubiquitin binding proteins resident in the clathrin pathway (31). Non-clathrin-dependent endocytosis through lipid raft and caveolar pathways has recently emerged as another important trafficking pathway6. Lipid rafts are cholesterol- and sphingolipid-rich domains in the membrane (32, 33), a subpopulation of which form membrane invaginations called caveolae that are rich in caveolin protein (34, 35). Lipid rafts and caveolae function in vesicular

and cholesterol trafficking (36, 37). The internalization pathway of LDLR remains unclear. Receptor internalization through the clathrin pathway may be important for LDLR recycling and LDL particle, LDLR complex has been found in early endosome antigen-1 (EEA1)-positive endosomes that are downstream of this route. However, caveolin-1 has been shown to bind CAP1 –PCSK9 complex (Figure5) and another study suggests that receptors can internalize through a non-clathrin-dependent pathway (38). Here we show that LDLR are internalized by both clathrin- and caveolae lipid raft-dependent pathways. PCSK9 dependent LDLR degradation is dependent on lipid raft-caveolar pathways (Fig 4E). We also identified that the multi-subunit protein CAP1 and PCSK9 are required for LDLR lysosomal sorting (Fig 4E). In this study, we confirmed that CAP1 alters PCSK9 mediated LDLR degradation; rather, exogenously added PCSK9 bound to CAP1 is still endocytosed and routed to lysosomes. Endocytosed LDLR predominantly follows the default recycling pathway back to the cell surface, so the means by which PCSK9 diverts LDLR to lysosomes remains an important question importantly, our study characterized PCSK9 interactions and trafficking under more

relevant physiological conditions. In addition to these localizations, we have newly identified that CAP1 is partially localized in the lipid rafts of plasma membrane. Lipid rafts are lipid microenvironments that contain high density of cholesterol and sphingolipid. These microdomains are specialized compartments serving as signaling platforms that facilitate signal transduction through concentrating the signaling molecules, or as insulators that separate the signaling molecules to their effectors (23). Among the various proteins interacted with caveolae, some isoforms of adenylyl cyclase (AC) are known to be specifically localized at these microdomains. Consistent with this idea, we found that siRNA knockdown of Cavelolin1 and CAP1 impairs PCSK9 endocytosis, LDLR degradation (Fig 2B, 4E). We therefore have showed that CAP1, caveolin 1 regulate PCSK9 endocytosis by affecting endocytic recruitment or receptor clustering. Consequently, we discovered a novel, caveolin 1-dependent interaction between PCSK9 and LDLR that facilitates LDLR lysosomal delivery and function. Based on our observations, we propose that PCSK9 is involved in a novel lysosomal transport complex that would allow it to degrade target of LDLR.

REFERENCES

1. Brown, M. S., and J.L. Goldstein. A receptor-mediated pathway for cholesterol homeostasis.*Science*.1986;232:34-47.

2. Goldstein, J.L., and M. S. Brown. The LDL receptor. *Arterioscler.Thromb.Vasc.Biol.*2009;29:431-438.

3. Park, S. W., Y. A. Moon, and J.D. Horton. Post-transcriptional regulation of low density lipoprotein receptor protein by proprotein convertase subtilisin/kexin type 9 in mouse liver. *J. Biol. Chem.*2009;279:50630-50638.

4. Benjannet, S., D. Rhainds, R, et al. NARC-1/PCSK9 and its natural mutants: zymogen cleavage and effects on the LDLR and LDL-cholesterol. *J. Biol. Chem.* 2004;279:48865-48875.

5. Maxwell, K. N., and J. L. Bresolw. Adenoviral-mediated expression of PCSK9 in mice results in a low-density lipoprotein receptor knockout phenotype. *Proc. Natl. Acad. Sci. USA.* 2004;101.7100-7105.

6. Herrington W, Lacey B, Sherliker P, Armitage J and Lewington S. Epidemiology of Atherosclerosis and the Potential to Reduce the Global Burden of Atherothrombotic Disease. *Circ Res*. 2016;118:535-46.

7. Pedersen TR. The Success Story of LDL Cholesterol

Lowering. *Circ Res*. 2016;118:721-31.

8. Jarcho JA and Keaney JF, Jr. Proof That Lower Is Better-LDL Cholesterol and IMPROVE-IT. *N Engl J Med*. 2015;372:2448-50.

9. Cannon CP, Blazing MA, Giugliano RP, McCagg A, White JA, Theroux P, Darius H, Lewis BS, Ophuis TO, Jukema JW, De Ferrari GM, Ruzyllo W, De Lucca P, Im K, Bohula EA, Reist C, Wiviott SD, Tershakovec AM, Musliner TA, Braunwald E, Califf RM and Investigators I-I. Ezetimibe Added to Statin Therapy after Acute Coronary Syndromes. *N Engl J Med*. 2015;372:2387-97.

10. Serban MC, Colantonio LD, Manthripragada AD, Monda KL, Bittner VA, Banach M, Chen L, Huang L, Dent R, Kent ST, Muntner P and Rosenson RS. Statin Intolerance and Risk of Coronary Heart Events and All-Cause Mortality Following Myocardial Infarction. *J Am Coll Cardiol*. 2017;69:1386-1395.

11. Burke AC, Dron JS, Hegele RA and Huff MW. PCSK9: Regulation and Target for Drug Development for Dyslipidemia. *Annu Rev Pharmacol Toxicol*. 2017;57:223-244.

12. Navarese EP, Kolodziejczak M, Schulze V, Gurbel PA, Tantry U, Lin Y, Brockmeyer M, Kandzari DE, Kubica JM,

D'Agostino RB, Sr., Kubica J, Volpe M, Agewall S, Kereiakes DJ and Kelm M. Effects of Proprotein Convertase Subtilisin/Kexin Type 9 Antibodies in Adults With Hypercholesterolemia: A Systematic Review and Meta-analysis. *Ann Intern Med*. 2015;163:40-51.

13. Lipinski MJ, Benedetto U, Escarcega RO, Biondi-Zoccai G, Lhermusier T, Baker NC, Torguson R, Brewer HB, Jr. and Waksman R. The impact of proprotein convertase subtilisin-kexin type 9 serine protease inhibitors on lipid levels and outcomes in patients with primary hypercholesterolaemia: a network meta-analysis. *Eur Heart J*. 2016;37:536-45.

14. Stein EA, Mellis S, Yancopoulos GD, Stahl N, Logan D, Smith WB, Lisbon E, Gutierrez M, Webb C, Wu R, Du Y, Kranz T, Gasparino E and Swergold GD. Effect of a monoclonal antibody to PCSK9 on LDL cholesterol. *N Engl J Med*. 2012;366:1108-18.

15. Seidah NG, Awan Z, Chretien M and Mbikay M. PCSK9: a key modulator of cardiovascular health. *Circ Res*. 2014;114:1022-36.

16. Cho Y, Lee SE, Lee HC, Hur J, Lee S, Youn SW, Lee J, Lee HJ, Lee TK, Park J, Hwang SJ, Kwon YW, Cho HJ, Oh BH,

Park YB and Kim HS. Adipokine resistin is a key player to modulate monocytes, endothelial cells, and smooth muscle cells, leading to progression of atherosclerosis in rabbit carotid artery. *J Am Coll Cardiol*. 2011;57:99-109.

17. Field J, Vojtek A, Ballester R, Bolger G, Colicelli J, Ferguson K, Gerst J, Kataoka T, Michaeli T, Powers S and et al. Cloning and characterization of CAP, the S. cerevisiae gene encoding the 70 kd adenylyl cyclase-associated protein. *Cell*. 1990;61:319-27.

18. Matviw H, Yu G and Young D. Identification of a human cDNA encoding a protein that is structurally and functionally related to the yeast adenylyl cyclase-associated CAP proteins. *Mol Cell Biol*. 1992;12:5033-40.

19. Bonifacino,J.S., and Traub, L. M. Signals for sorting of transmembrane proteins to endosomes and lysosomes. *Annu. Rev. Biochem.* 2003; 72:395-447.

20. Lee S, Lee HC, Kwon YW, Lee SE, Cho Y, Kim J, Lee S, Kim JY, Lee J, Yang HM, Mook-Jung I, Nam KY, Chung J, Lazar MA and Kim HS. Adenylyl cyclase-associated protein 1 is a receptor for human resistin and mediates inflammatory actions of human monocytes. *Cell Metab*. 2014;19:484-97.

21. Bertling E, Hotulainen P, Mattila PK, Matilainen T, Salminen M and Lappalainen P. Cyclase-associated protein 1 (CAP1) promotes cofilin-induced actin dynamics in mammalian nonmuscle cells. *Mol Biol Cell*. 2004;15:2324-34.

22. Lagace , T. A. , D. E. Curtis , R. Garuti , M. C. McNutt , S. W. Park ,H. B. Prather , N. N. Anderson , Y. K. Ho , R. E. Hammer , and J.D. Horton. Secreted PCSK9 decreases the number of LDL receptoreceptors in hepatocytes and in livers of parabiotic mice. *J. Clin.Invest*, 2006;116 : 2995 - 3005.

23. Maxwell , K. N. , E. A. Fisher , and J. L. Breslow Overexpressionof PCSK9 accelerates the degradation of the LDL receptor in a postendoplasmic reticulum compartment. *Proc. Natl. Acad. Sci. USA*..2005; 102 : 2069 - 2074 .

24. Brautbar, A. & Ballantyne, C. M. Pharmacological strategies for lowering LDL cholesterol: statins and beyond. *Nat. Rev. Cardiol*. 2011; 8: 253-265.

25. Wijers, M., Kuivenhoven, J. A. & van de Sluis, B. The life cycle of the low-density lipoprotein receptor: insights from cellular and in-vivo studies.

26. Eric N. Hampton, Mark W. Knuth, Jun Li, Jennifer L. Harris, Scott A. Lesley, and Glen Spraggon. The self-inhibited

structure of full-length PCSK9 at 1.9 Å reveals structural homology with resistin within the C-terminal domain. *Proc. Natl. Acad. Sci. USA.* 2007; 104: 37,14604-14609

27. Simons, K., and Toomre, D. Lipid rafts and signal transduction. *Nature reviews Molecular cell biol.* 2000;1:31-27.

Jeong H, Lee H, Kim K, Kim K, Yoon D, Park S. Sterol-dependent regulation of proprotein convertase subtilisin/kexin type 9 expression by sterol-regulatory element binding protein-2. *Journal of Lipid Research.*2008;49:399-409.

28. Gruenberg, J. The endocytic pathway: a mosaic of domains. *Nature Rev. Mol. Cell Biol.* 2001; 2, 721-730

29. Baass, P. C., Di Guglielmo, G. M., Authier, F., Posner, B. I. & Bergeron, J. J. M. Compartmentalized signal transduction by tyrosine kinases. *Trends Cell Biol.* 1995; 5, 465-470

30. Di Fiore, P. P. & De Camilli, P. Endocytosis and signaling. an inseparable partnership. *Cell.*2001; 106, 1-4

31. McPherson, P. S., Kay, B. K. & Hussain, N. K. Signaling on the endocytic pathway. *Traffic* .2001; 2, 375-384

32. Katzmann, D. J., Babst, M. & Emr, S. D. Ubiquitin-dependent sorting into the multivesicular body pathway requires the function of a conserved endosomal protein sorting

complex, ESCRT-I. *Cell* .2001;106, 145-155

33. Sharma, P., Sabharanjak, S. & Mayor, S. Endocytosis of lipid rafts: an identity crisis. *Sem. in Cell Dev. Biol.* 2002; 13, 205-214

34. Anderson, R. G. & Jacobson, K. A role for lipid shells in targeting proteins to caveolae, rafts, andother lipid domains. *Science* .2002; 296, 1821-1825

35. Simons, K. & Toomre, D. Lipid rafts and signal transduction. *Nature Rev. Mol. Cell Biol.* 2000;1, 31-39

36. Anderson, R. G., Kamen, B. A., Rothberg, K. G. & Lacey, S. W. Potocytosis: sequestration and transport of small molecules by caveolae. *Science* .1992; 255, 410-411

37. Razani, B., Schlegel, A. & Lisanti, M. P. Caveolin proteins in signaling, oncogenic transformation and muscular dystrophy. *J. Cell Sci.* 2000; 113, 2103-2109

38. Zwaagstra, J. C., El-Alfy, M. & O'Connor-McCourt, M. D. Transforming growth factor (TGF)-β 1 internalization: modulation by ligand interaction with TGF-β receptors types I and II and a mechanism that is distinct from clathrin-mediated endocytosis. *J. Biol. Chem.* 2001; 276, 27237-27245

39. Schroeder, C.I., Swedberg, J.E., Withka, J.M., Rosengren,

K.J., Akcan, M., Clayton, D.J., Daly, N.L., Cheneval, O., Borzilleri, K.A., Griffor, M., Stock, I., Colless, B., Walsh, P., Sunderland, P., Reyes, A., Dullea, R., Ammirati, M., Liu, S., McClure, K.F., Tu, M., Bhattacharya, S.K., Liras, S., Price, D.A., Craik, D.J. Design and synthesis of truncated EGF-A peptides that restore LDL-R recycling in the presence of PCSK9 in vitro. *Chem.Biol.* 2014;21: 284-294.

40. Chen, R., Li, L., and Weng, Z. ZDOCK: an initial-stage protein-docking algorithm. *Proteins.* 2003; 52, 80-87.

41. Chen, R., and Weng, Z. A novel shape complementarity scoring function for protein-protein docking. *Proteins*. 2003;51, 397-408.

42. Zoete, V., Irving, M.B., and Michielin, O. MM-GBSA binding free energy decomposition and T cell receptor engineering. *J. Mol. Recognit.* 2010;23, 142-152.

국문 초록

서론: Proprotein convertase subtilisin/kexin type 9 (PCSK9)은 간에서 분비되고 LDLR (LDL receptor)의 내인성 억제제로서 콜레스테롤 항상성의 핵심 조절인자이다. PCSK9은 세포막에 존재하는 LDLR의 EGF-A 도메인과 결합하여 세포 내로 이동한 후, 세포 내 LDLR이 라이소좀(lysosome)에서 분해될 수 있도록 하는 단백질로, PCSK9과 LDLR의 결합을 억제해 LDLR 양이 증가되면 혈중 콜레스테롤 농도가 감소하는 것으로 알려졌다. 하지만, PCSK9과 LDLR이 결합되어, LDLR이 분해되는 기작과 재활용되어 콜레스테롤이 조절되는 기작의 선별적 특이성에 대한 보고는 없었다.

방법: 대사성 질환과 염증성 질환 모두에서 높게 측정되는 바이오마커 리지스틴(resisitn)과 PCSK9구조의 유사함이 보고된바 있고, Adenlylyl cyclase-associated protein(CAP1)이 리지스틴의 수용체인 것을 밝힌 이전의 보고를 바탕으로, CAP1이 또한 PCSK9의 수용체일 것이라 예상하고, in vitro binding assay, SPR, virtual modeling을 수행하였다. 이와 더불어, TALEN-mediated CAP1 knockout mice 제작 및 in vitro, in vivo assay를 실시하여, PCSK9 mediated LDL receptor 분해 기전을 밝혔다.

결과: 다양한 binding assay를 실시하여, 우리는 CAP1과 PCSK9 trimers가 binding하는 결과를 얻었다. 이는 CAP1-SH3

domain(Proline rich SH3 binding domain)과 PCSK9-CHRD (Cystein-Histidine rich domain) 이 직접적으로 결합하고, 이렇게 생성된 구조물은 Lysosome으로 LDLR를 운송하여, 분해한다. 특히, 이 분해 기작에 caveolin1이 주요하게 작용하여, 이전의 주장과 다르게 원형질막에서 유래된 lipid-raft를 통해 이루어짐을 확인하였다. 이에, CAP1 특이적 siRNA를 HepG2세포주에서 발현시켜, CAP1의 발현을 억제 시키자, LDLR가 분해되지 않았고. caveolin1의 발현을 억제시켜도 동일한 결과를 얻어, LDLR 분해 기작에 CAP1, caveolin 1 이 관여함을 밝혔다. 탈렌 CAP1 knockout 마우스의 지질프로파일을 분석결과, plasma LDL cholesterol (Low density lipoprotein cholesterol)농도가 컨트롤 개체에 비해 낮고, large HDL cholesterol (High density lipoprotein cholesterol)의 비율이 높게 나타나는 개선된 결과를 보였다.

결론: 기존의 clathrin 매개 endocytotic LDLR (LDL cholesterol 수용체) 분해 방식이 아니라, caveolae을 통해 PCSK9이 LDLR를 lysosome에서 분해를 하는 새로운 기전을 밝혔다. 특히, CAP1이 새로운 PCSK9의 수용체임을 밝히고, PCSK9/ LDLR/ CAP1/ caveolin 1 복합체가 형성되어, lysosome에서 LDLR 분해가 이루어진다. 또한 CAP1을 제거한 형질 전환 마우스는 LDLR 수준이 증가하여 LDL cholesterol의 제거가 가속화됨으로써 콜레스테롤의 혈중농도가 감소하는 결과를 얻었다. 이상의 연구결과를 종합적으로

CAP1이 PSCK9의 새로운 수용체로, LDLR의 분해 기작에 주요한 역할을 하는 것을 밝혀냈다.

주요어; Proprotein convertase subtilisin/kexin type 9 (PCSK9), LDL receptor (LDL receptor), Adenlylyl cyclase-associated protein(CAP1), Caveolin1, PCSK9 mediated LDL receptor 분해 기전

학 번; 2009-31343